

AD _____

Award Number: W81XWH-FE0001

TITLE: O&C of the Army Medical Research and Materiel Command

PRINCIPAL INVESTIGATOR: U.S. Army Medical Research and Materiel Command

CONTRACTING ORGANIZATION: T[] of the Army Medical Research and Materiel Command, Fort Detrick, Maryland 21702-5012

REPORT DATE: June 2000

TYPE OF REPORT: Annual

PREPARED FOR: U.S. Army Medical Research and Materiel Command
Fort Detrick, Maryland 21702-5012

DISTRIBUTION STATEMENT: Approved for public release; distribution unlimited

The views, opinions and/or findings contained in this report are those of the author(s) and should not be construed as an official Department of the Army position, policy or decision unless so designated by other documentation.

REPORT DOCUMENTATION PAGE				Form Approved OMB No. 0704-0188	
Public reporting burden for this collection of information is estimated to average 1 hour per response, including the time for reviewing instructions, searching existing data sources, gathering and maintaining the data needed, and completing and reviewing this collection of information. Send comments regarding this burden estimate or any other aspect of this collection of information, including suggestions for reducing this burden to Department of Defense, Washington Headquarters Services, Directorate for Information Operations and Reports (0704-0188), 1215 Jefferson Davis Highway, Suite 1204, Arlington, VA 22202-4302. Respondents should be aware that notwithstanding any other provision of law, no person shall be subject to any penalty for failing to comply with a collection of information if it does not display a currently valid OMB control number. PLEASE DO NOT RETURN YOUR FORM TO THE ABOVE ADDRESS.					
1. REPORT DATE (DD-MM-YYYY) 01-06-2011		2. REPORT TYPE Annual		3. DATES COVERED (From - To) 17 MAY 2010 - 16 MAY 2011	
4. TITLE AND SUBTITLE Discovery and Testing of Ricin Therapeutics				5a. CONTRACT NUMBER	
				5b. GRANT NUMBER W81XWH-10-2-0048	
				5c. PROGRAM ELEMENT NUMBER	
6. AUTHOR(S) Professor Domenico Tortorella E-Mail: domenico.tortorella@mssm.edu				5d. PROJECT NUMBER	
				5e. TASK NUMBER	
				5f. WORK UNIT NUMBER	
7. PERFORMING ORGANIZATION NAME(S) AND ADDRESS(ES) Mount Sinai School of Medicine of New York New York, NY 10029				8. PERFORMING ORGANIZATION REPORT NUMBER	
9. SPONSORING / MONITORING AGENCY NAME(S) AND ADDRESS(ES) U.S. Army Medical Research and Materiel Command Fort Detrick, Maryland 21702-5012				10. SPONSOR/MONITOR'S ACRONYM(S)	
				11. SPONSOR/MONITOR'S REPORT NUMBER(S)	
12. DISTRIBUTION / AVAILABILITY STATEMENT Approved for Public Release; Distribution Unlimited					
13. SUPPLEMENTARY NOTES					
14. ABSTRACT Ricin is an extremely potent A-B toxin that is transported from the cell surface to the cytosol where it inactivates ribosomes leading to cell death. Ricin access to the cytosol is dependent on its transport from the cell surface to the ER lumen. An elegant human cell system that specifically examines ricin A chain dislocation across the ER bilayer has been established. Using enzymatic attenuated ricin A chain molecules (RTAE177D and RTA!), ricin A chains undergo a rapid transport across the ER membrane and into cytosol where it is eventually degraded by the proteasome. The transport of the ricin A chain occurred via a membrane associated intermediate and likely utilizes some components of ER quality control. These assays demonstrate that ricin A chain is an unstable molecule whose instability will be utilized in a high-throughput screen to identify chemicals that block ricin transport, thus stabilizing the ricin molecule. A green fluorescent protein ricin chimeras that allow for more efficient screening have been generated and optimized to create a very robust high-throughput screen. These cells expressing the fluorescent ricin molecule will be utilized to discover novel inhibitors that block ricin intoxication.					
15. SUBJECT TERMS Ricin toxin, dislocation, small weight compounds, chemical inhibitors, high-throughput screen, fluorescent-based cell assay					
16. SECURITY CLASSIFICATION OF:			17. LIMITATION OF ABSTRACT	18. NUMBER OF PAGES	19a. NAME OF RESPONSIBLE PERSON
a. REPORT	b. ABSTRACT	c. THIS PAGE			USAMRMC
U	U	U	UU	20	19b. TELEPHONE NUMBER (include area code)

Table of Contents

	Page
Introduction.....	4
Body.....	4-10
Key Research Accomplishments.....	11
Reportable Outcomes.....	11
Conclusion.....	11
References.....	11-12
Appendices.....	12-20

INTRODUCTION:

Ricin toxin is an extremely toxic polypeptide found in castor beans (*Ricinus communis*) (1). Ricin is a heterodimer comprised of a catalytically active polypeptide (A chain or RTA) covalently linked by a disulfide bond to a lectin binding B subunit (RTB). Galactose-specific lectin binding domain of the B chain enables ricin toxin to interact with cell surface glycolipids and glycoproteins (2). This allows the A-B hetero-dimer to enter the cell via endocytosis and be transported to the endoplasmic reticulum (ER) lumen. While in the ER, the ricin A chain co-opts ER quality control to gain access to the cytosol by a process referred to as dislocation or retrograde translocation (3). Once in the cytosol, the A chain inactivates the ribosome, halting protein synthesis that eventually leads to cell death. The A chain gains access to the

Ricin is a member of the A-B family of toxins (e.g. shiga, cholera, pseudomonas exotoxin A, or pertussis toxin) that is transported from the cell surface to the ER lumen and ultimately into the cytosol (4). ER quality control normally scrutinizes nascent polypeptides and disposes of misfolded proteins by proteasome destruction (5). Upon arrival of the ricin toxin in the ER, the ER chaperones protein disulfide-isomerase (PDI) and calreticulin are proposed to play a role in ricin transport across the ER membrane. PDI likely reduces the disulfide bond that covalently links the A-B chains causing release of the active A-chain (6, 7), while calreticulin activity would assist the structural changes of the toxin prior to its dislocation (8). Moreover, the ER degradation enhancing α -mannosidase I-like protein involved in degradation of misfolded ER proteins (9) also plays a role in ricin dislocation from the ER to the cytosol (10). Subsequently, the toxin may be extracted through the membrane via the Sec61 translocon (11). In addition, Hsc70 cytosolic chaperone machinery protects ricin A chain from the Hsp90 assisted cytosolic degradation (12). Collectively, these findings demonstrate that ricin utilizes multiple cellular factors for its transport across the ER bilayer. Despite these findings, the molecular mechanism of ricin dislocation has yet to be fully defined.

The potency of ricin to inactivate 2,000 ribosomes/minute precludes the need for a large number of molecules to reach the cytoplasm (13, 14). Even though the enzymatic properties of ricin have been delineated in detail, the actual export of the ricin A chain across the ER membrane and into the cytosol is only currently being characterized (15). Hence, the current project aims to identify inhibitors that block the critical step of ricin transport into the cytosol.

BODY:

Ricin A chains directed to the ER block protein synthesis.

The investigation of ricin toxin transport across the ER membrane has been hampered by the low number of toxin molecules that reach the ER lumen when added extracellularly (11). Hence, we aimed to

create a human cell-based assay to specifically study RTA transport across the ER membrane. In line with this objective, we initially confirmed that RTA molecules directed to the ER (16, 17) in human cells limited protein expression. Full length wild-type RTA (FL-RTA_{WT}) and wild-type mature RTA equipped with a murine MHC class I molecule (K^b) signal peptide and an HA epitope tag at its N-terminus (RTA_{WT}) were co-transfected with a GFP expression plasmid in HEK-293T cells and evaluated for GFP fluorescence using flow cytometry (Figure 1A-D). The lack of GFP fluorescent cells is indicative of functionally active RTA molecules. FL-RTA_{WT} and RTA_{WT} limited the expression of GFP in a significant percentage of cells (Figure 1C and D, 2% and 15%, respectively) when compared to cells

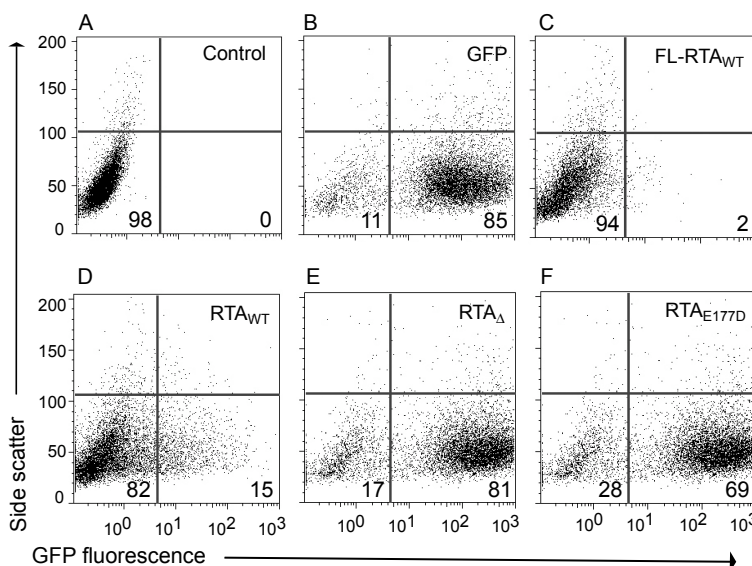


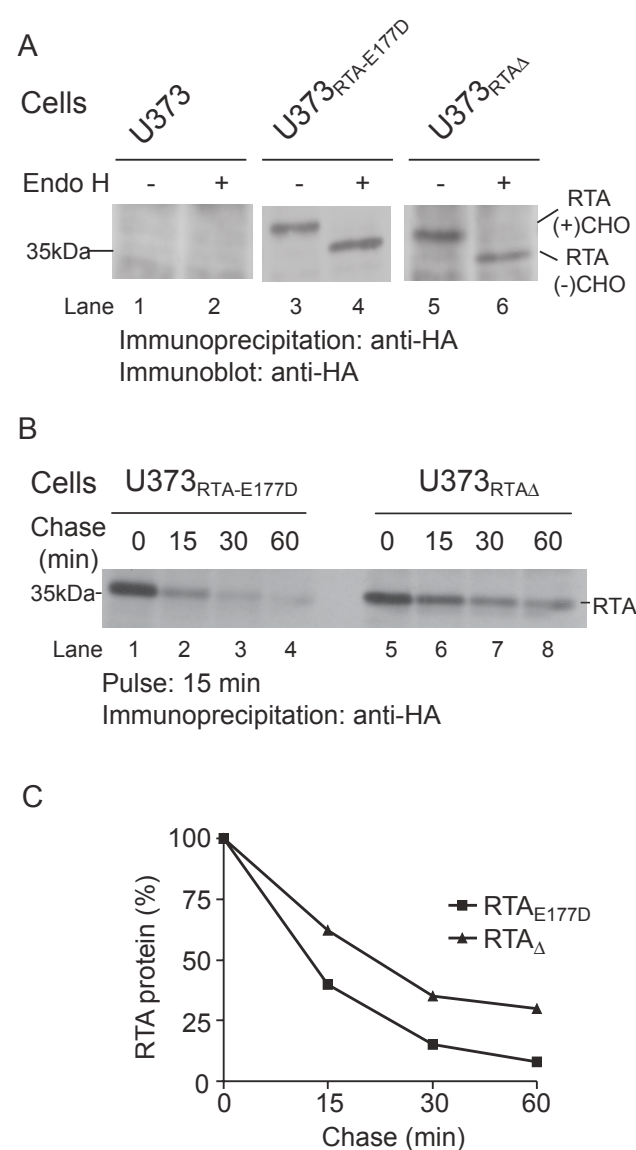
Figure 1. RTA inhibits protein expression in human cells. HEK-293T cells transfected with empty plasmid (Control, A) or a GFP-expressing plasmid (B) with full length wild type RTA (FL-RTA_{WT}) (C), RTA_{WT} (D), RTA_Δ (E), and RTA_{E177D} (F) were analyzed for GFP expression using flow cytometry. The values in the quadrants represent percentage of total cells.

transfected with GFP alone (Figure 1B, 85%). These data suggest that ER

directed RTA molecules are dislocated across the ER and to the cytosol where they inhibit protein synthesis.

Ricin A chain expression in human cells

Due to the toxic nature of wild type RTA, we cloned ricin A chain mutants (RTA_{E177D} and RTA_Δ,



Experimental Procedures) that are enzymatically attenuated to study A chain dislocation (18, 19). RTA_{E177D} is a site-directed mutant with attenuated activity that is structurally similar to wild type (20), while RTA_Δ has deletion of residues 177-181. These constructs like RTA_{WT} were also engineered with the N-terminal K^b signal peptide and HA epitope tag. An initial experiment was performed to determine whether RTA_{E177D} and RTA_Δ inhibit protein synthesis. GFP positive cells were examined in HEK-293T cells co-transfected with RTA_{E177D} and RTA_Δ and a GFP expression plasmid (Figure 1E-F). The RTA mutants, RTA_{E177D} and RTA_Δ had a diminished ability to affect GFP expression (Figure 1E-F) with RTA_{E177D} retaining some capacity to inhibit GFP expression. These data demonstrate that ricin A chain

mutants have limited capacity to prevent protein expression.

In order to study RTA dislocation, human U373 cells that stably express RTA_{E177D} and RTA_Δ (Experimental Procedures) (Figure 2) were created. Our initial experiment examined the acquisition of an N-linked glycan onto RTA_{E177D} and RTA_Δ to confirm their localization to the ER. RTA_{E177D} and

Figure 2. RTA polypeptides are unstable ER proteins. (A) U373, U373_{RTA-E177D}, and U373_{RTAΔ} cell lysates were incubated with anti-HA antibodies. The recovered precipitates were subjected to endoglycosidase H (Endo H) digestion and analyzed by immunoblot analysis. (B) U373_{RTA-E177D} and U373_{RTAΔ} cells were pulsed with ³⁵S-methionine for 15 min and chased for up to 60 min. The recovered RTA polypeptides were resolved by SDS-PAGE and detected by autoradiography. (C) Levels of RTA polypeptides were quantified by densitometry and plotted as a percentage to the 0 min chase point (100%). RTA polypeptides and molecular weight markers are indicated.

RTA_Δ molecules recovered from these cells were subjected to Endo H treatment followed by immunoblot analysis (Figure 2A). Endo H preferentially cleaves immature high mannose containing N-linked oligosaccharides characteristic of ER-resident molecules (21). RTA_{E177D} and RTA_Δ polypeptides with the predicted molecular weight were recovered from cell lysates (Figure 2A, lanes 3 and 5). As expected, faster migrating RTA polypeptides were observed upon treatment with Endo H (Figure 2A, lanes 2, 4, and 6). The difference in the relative molecular weight of the two species (~3-4 kDa) confirmed that the RTA polypeptides acquired a single N-linked glycan and were retained in the ER. These data demonstrate that this human cell-based assay can be utilized to study ricin dislocation.

Ricin A chains are subjected to proteasome degradation.

We next investigated the stability of the RTA polypeptides in U373_{RTA-E177D} and U373_{RTAΔ} cells by pulse-chase analysis (Figure 2B and C). The cells were metabolically labeled with ³⁵S-methionine for 15 min and

chased up to 60 min. Strikingly, the half-life of RTA_{E177D} (<10 min) was less than RTA_Δ (~ 20 min) (Figure 2B, lanes 1-8 and 2C). Given that ricin utilizes ER quality control to gain access to the cytosol (3, 22), it is expected that a population of ricin would be degraded. However, the rapid half-life of RTA_{E177D} expressed in human cells when compared to yeast (17,

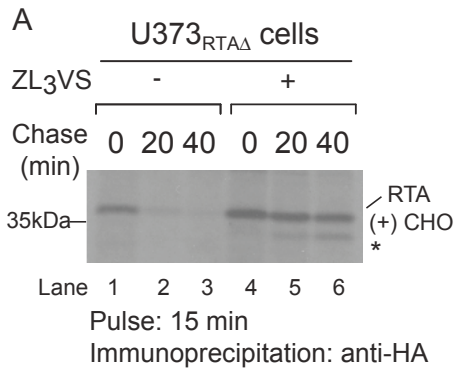
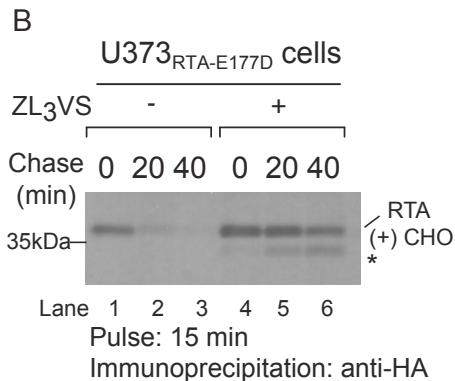


Figure 3. RTA polypeptides are stabilized in the presence of proteasome inhibitor. U373_{RTA_Δ} (A) and U373_{RTA-E177D} (B) cells treated with or without proteasome inhibitor (ZL₃VS) were pulsed with ³⁵S-methionine for 15 min and chased for up to 40 min. RTA polypeptides were recovered with an anti-HA antibody, resolved by SDS-PAGE, and detected by autoradiography. RTA polypeptides and molecular weight markers are indicated. * Indicates faster migratory species.



22) and plant cells (23, 24) suggests that RTA is efficiently transported out of the ER in human cells.

Are RTA polypeptides targeted for proteasome dependent degradation? To address this question, U373_{RTA-E177D} and U373_{RTA_Δ} cells treated with or without proteasome inhibitor carboxybenzyl-leucyl-leucyl-leucyl vinyl sulfone (ZL₃VS) (25 μM, 1 hr) were subjected to pulse-chase analysis (Figure 3). As expected, RTA polypeptides decreased over the chase period (Figure 3A and B, lanes 1-3). Strikingly, the inclusion of proteasome inhibitor stabilized both RTA_{E177D} and RTA_Δ molecules (Figure 3A and B, lanes 4-6). In addition, proteasome inhibition enabled the recovery of a faster migrating polypeptide intermediate (*) during the chase, most likely deglycosylated RTA species (Figure 3A and B, *, lanes 4-6). Collectively, the data demonstrate that ricin A chains are eventually

degraded in a proteasome dependent manner.

Characterization of RTA_{E177D} and RTA_Δ intermediates.

We next optimized conditions to observe the faster migrating RTA species. Total cell lysates from U373_{RTA-E177D} and U373_{RTA_Δ} cells treated with proteasome inhibitor ZL₃VS (10 μM) for up to 5 hours were subjected to immunoblot analysis (Figure 4A). Strikingly, RTA_{E177D} proteins were almost completely converted to the faster migrating species after 2 hrs of ZL₃VS treatment (Figure 4A, lanes 9-12). In contrast, RTA_Δ molecules displayed a biphasic conversion in which an increase in glycosylated RTA_Δ was observed during the early times of proteasome inhibition (Figure 4A, lanes 2-3) followed by an accumulation of glycosylated and faster migrating species during later times of ZL₃VS treatment (Figure 4A, lanes 4-6). Interesting, the ratio of glycosylated (RTA(+))CHO to faster migrating species following proteasome treatment significantly varied between the RTA mutants (Figure 4A, lanes 1-6 and 7-12, respectively). These results suggest that RTA_{E177D} and RTA_Δ are likely processed differently due to the folding status of the polypeptide.

To address the N-linked glycosylation status of the RTA_Δ and RTA_{E177D} intermediates, we examined their sensitivity to *in vitro* glycosidase treatment (Figure 4B). RTA polypeptides recovered from U373_{RTA-E177D} and U373_{RTA_Δ} cells treated with proteasome inhibitor (2.5 μM, 10 hours) were undigested or digested with EndoH (EH) or peptide N-glycanase (PNGase or PN) followed by immunoblot analysis (Figure 4B). U373 cells were used as a negative control. As expected, two species of RTA polypeptides were observed exclusively from proteasome-inhibitor treated cells (Figure 4B, lanes 10 and 16). Moreover, only the slower migrating glycosylated species were sensitive to EndoH and PNGase digestion resulting in the faster migrating form of the RTA-reactive polypeptides (Figure 4B, lanes 11-12 and 17-18). Calnexin levels demonstrated equivalent protein loading (Figure 4B, lanes 19-36). These data suggest that the faster migrating RTA species are deglycosylated intermediates generated from the dislocation of ricin polypeptides.

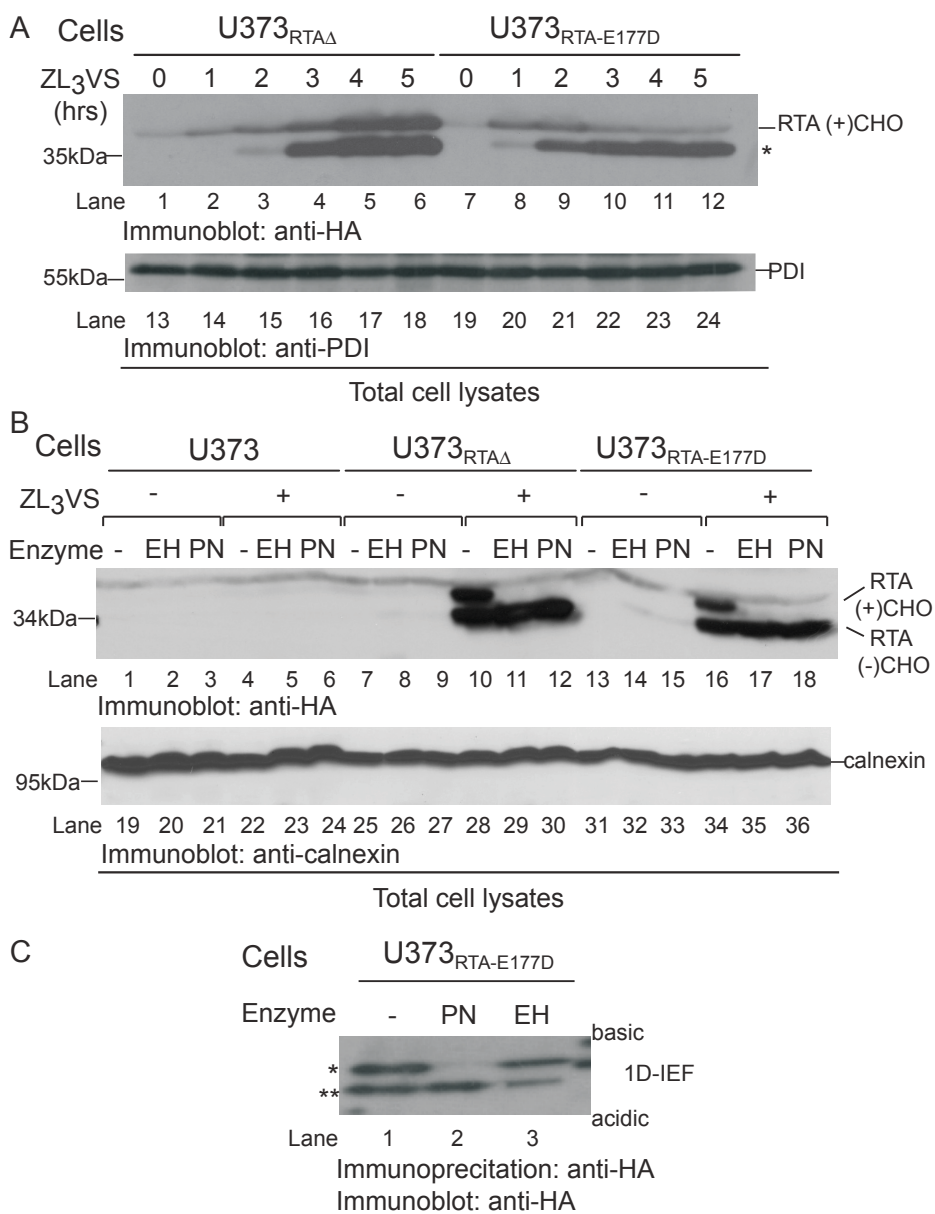


Figure 4. RTA molecules accumulate as deglycosylated intermediates. (A) $U373_{RTA\Delta}$ and $U373_{RTA-E177D}$ cells treated with ZL₃VS for up to 5 hrs were subjected to immunoblot analysis for RTA (lanes 1-12) and PDI (lanes 13-24). (B) Total cell lysates from $U373$, $U373_{RTA-E177D}$, and $U373_{RTA\Delta}$ cells untreated or treated with proteasome inhibitor were subjected to endoglycosidase H (EH), or peptide N-glycanase (PN). Immunoblot analysis was performed for RTA (lanes 1-18) and calnexin (lanes 19-36) proteins. (C) RTA polypeptides recovered from $U373_{RTA-E177D}$ cells treated with ZL₃VS were subjected to PN or EH treatment. Subsequently, the samples were resolved by one-dimensional isoelectric focusing (1D-IEF) and subjected to immunoblot analysis. The respective polypeptides and molecular weight markers are indicated. *Indicates faster migrating species.

In order to confirm that the N-terminal epitope tag does not affect the processing of the RTA polypeptides, we examined the accumulation of untagged RTA mutants upon proteasome inhibition (Supporting Data Figure 1). Cell lysates from proteasome inhibitor treated $U373$, $U373_{RTA-E177D}$, $U373_{KbRTA\Delta}$, and $U373_{KbRTA-E177D}$ cells were subjected to immunoblot analysis. Two species of RTA molecules, glycosylated and deglycosylated, accumulated in proteasome inhibitor treated cells; a result demonstrating that the stability of both forms of RTA is independent of the N-terminus epitope tag.

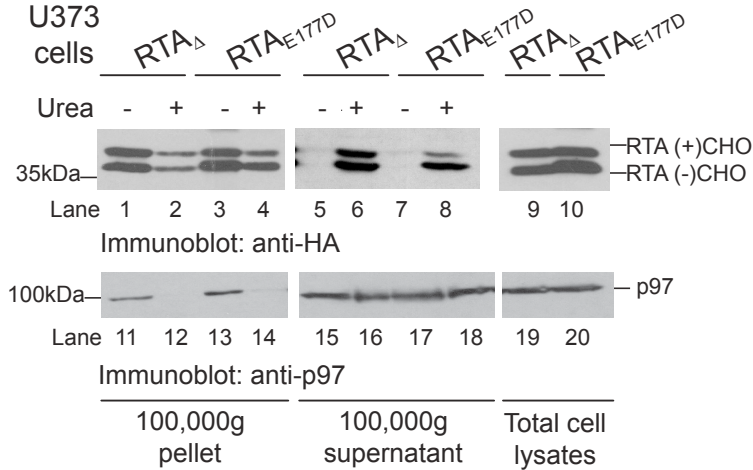
To confirm that the faster migrating RTA species were indeed digested by cellular PNGase, the RTA polypeptides were resolved on a 1D-IEF gel. PNGase cleavage results in the conversion of asparagine to aspartic acid causing a more acidic species, thus changing the overall charge of the polypeptide (25). RTA polypeptides recovered from $U373_{RTA-E177D}$ cells treated with proteasome inhibitor (2.5 μ M, 10 hours) were untreated or treated with EndoH or PNGase, resolved on a 1D-IEF gel and subjected to immunoblot analysis (Figure 4C). RTA_{E177D} polypeptides

from ZL₃VS-treated cells migrated as two discrete bands likely corresponding to species with different charges (Figure 4C, lane 1, * and **). Strikingly, *in vitro*

PNGase digestion of RTA_{E177D} polypeptides caused the polypeptides to migrate at a similar position as the more acidic RTA molecules (Figure 4C, lane 2, **), while EndoH treatment did not alter the migration pattern of the RTA_{E177D} polypeptides (Figure 4C, lane 3). The same result was observed for RTA_A². These results demonstrate that RTA polypeptides are subjected to cellular deglycosylation during dislocation.

Ricin A chains utilize ER membrane factors for efficient dislocation.

To characterize the membrane topology of stabilized RTA polypeptides, we performed a subcellular fractionation protocol (26). Membrane microsomes from U373_{RTA-E177D} and U373_{RTA Δ} cells treated with



proteasome inhibitor (2.5 μ M, 10 hrs) were incubated with 4.5M urea and subjected to high-speed centrifugation (100,000g) to separate the membrane fraction from the supernatant fraction. The 100,000g supernatant, 100,000g pellet, and total cell lysates were subjected to immunoblot analysis for RTA mutants (Figure 5, lanes 1-10) and p97 (Figure 5, lanes 11-20). The p97 polypeptide is a soluble cytosolic protein that associates with the ER membrane (27) and as expected, was completely extracted from the bilayer upon treatment with urea (Figure 5, lanes 12 and 14). As expected, some of the stabilized RTA_{E177D} and RTA Δ molecules were found in the

Figure 5. *RTA dislocation utilizes membrane components.* Microsomal preparation from subcellular homogenates of U373_{RTA Δ} and U373_{RTA-E177D} cells were treated with or without 4.5 M urea and centrifuged at 100,000g. Total cell lysates, 100,000g pellets, and the 100,000g supernatant were subjected to immunoblot analysis against RTA (lanes 1-10) and p97 (lanes 11-20). The respective polypeptides and molecular weight markers are indicated.

100,000g supernatant (Figure 5, lanes 6 and 8). Strikingly, a significant population of RTA_{E177D} and RTA Δ was observed with the membrane fraction (Figure 5, lanes 2 and 4) demonstrating that these

RTA molecules are integrated into the bilayer. These results imply that ricin A chains are efficiently dislocated via membrane-integrated intermediates.

Ricin A chains are dislocated utilizing selective components of ER quality control.

To validate that RTA polypeptides were dislocated utilizing the ER quality control machinery, we examined the effect of a dislocation inhibitor, eeyarestatin I (28), on the stability of ricin A chains. U373_{RTA-E177D} and U373_{RTA Δ} cells treated with or without eeyarestatin (5mg/mL) or the proteasome inhibitor ZL₃VS (2.5 μ M) were subjected to immunoblot analysis (Figure 6A). PDI levels assured equivalent protein loading (Figure 6A, lanes 9-16). As expected, treatment with ZL₃VS caused a significant increase in both RTA Δ and RTA_{E177D} polypeptides (Figure 6A, lanes 5-8) with a difference between the levels of glycosylated (RTA(+)_{CHO}) and deglycosylated (RTA(-)_{CHO}) molecules. Interestingly, mostly glycosylated RTA Δ and RTA_{E177D} polypeptides accumulated from cells treated with eeyarestatin I (Figure 6A, lanes 2 and 4). However, since eeyarestatin I attenuates the process of dislocation and not proteasome function (28), it was interesting that deglycosylated forms of the ricin A chain were observed (Figure 6A, lanes 2 and 4). Therefore, ricin A chain dislocation probably occurs using a distinct mechanism compared to ERAD substrates.

To further explore the involvement of dislocation-associated cellular proteins in the transport of ricin toxin across the ER membrane, we investigated the role of SEL1L and Derlin-1 in the dislocation of RTA_{E177D} and RTA Δ polypeptides. SEL1L functions as part of the mammalian Hrd1 ligase complex and is proposed to be involved in the recognition of ER degradation substrates (29, 30). Derlin-1 plays a role in the extraction of certain misfolded ER proteins and a dominant negative form, Derlin-1-gfp can impede substrate dislocation (31-33). U373_{RTA-E177D} and U373_{RTA Δ} transduced with Derlin1-gfp and shRNA against SEL1L were untreated or treated with ZL₃VS (2.5 μ M, 10 hrs) and subjected to immunoblot analysis (Figure 6B). The expression of the constructs was confirmed using anti-SEL1L (Figure 6B, lanes 13-24) and anti-GFP (Figure 6B, lanes 25-36) immunoblots. Derlin1-gfp expression did not alter the levels of RTA polypeptides regardless of proteasome inhibition (Figure 6B, lanes 1-2, 4-5, 7-8, and 10-11). These results are consistent with published findings implicating that ricin toxin transport across the ER membrane is Derlin-1 independent (10). On the other hand, silencing of SEL1L resulted in a substantial increase of RTA polypeptides in both the presence and absence of proteasome inhibition (Figure 6B, lanes 3, 6, 9, 12). Anti-GAPDH immunoblot indicates equal protein loading

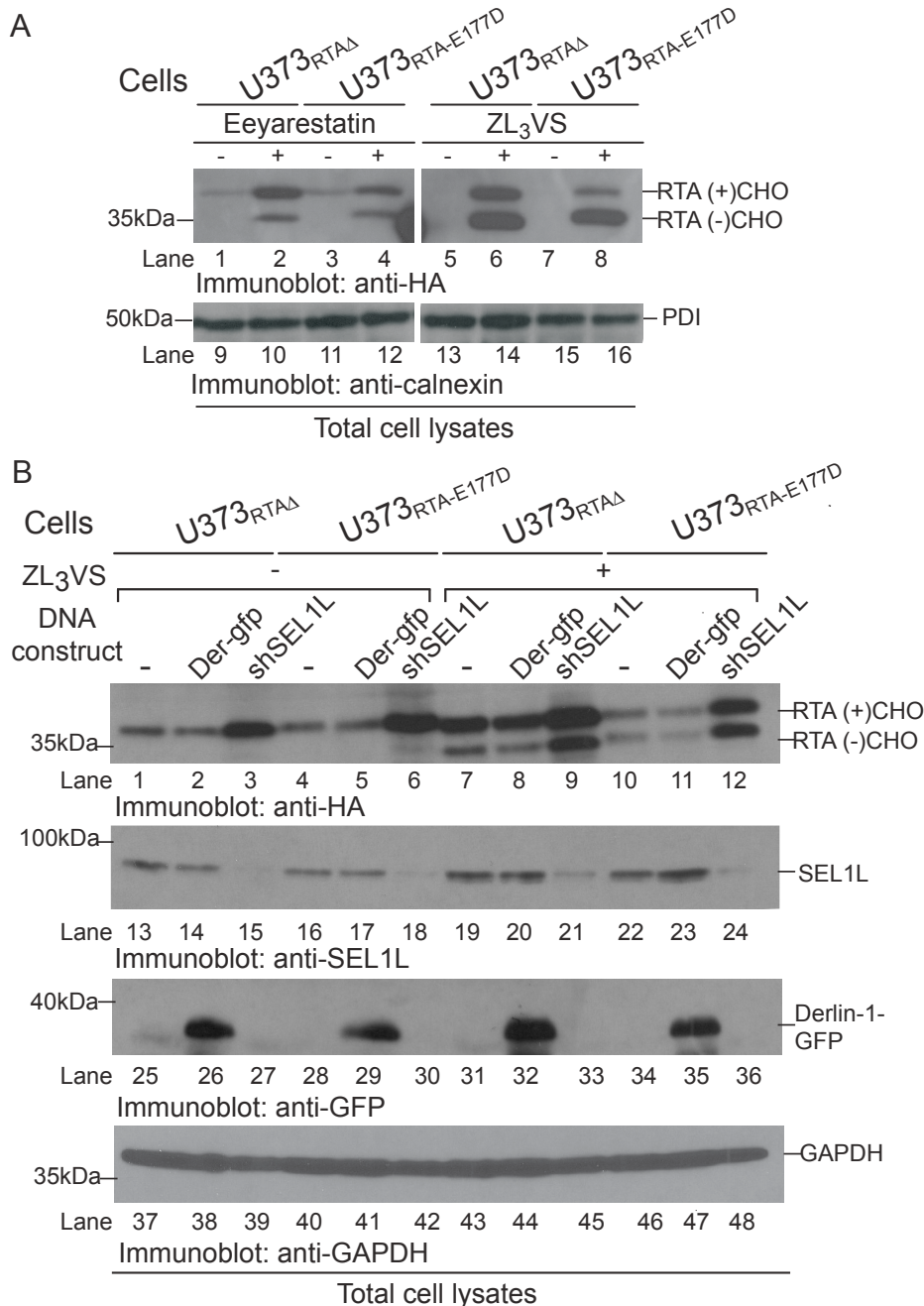


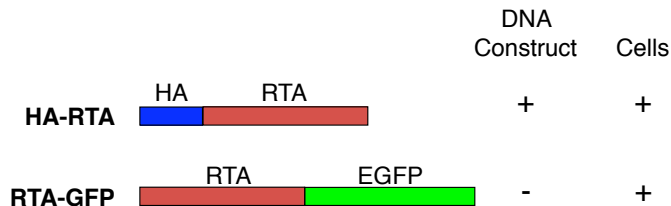
Figure 6. RTA is dislocated utilizing selective ER proteins. (A) U373_{RTAΔ} and U373_{RTA-E177D} cells untreated or treated with eeyarestatin I and ZL₃VS were subjected to immunoblot analysis for RTA (lanes 1-8) and PDI (lanes 9-16) polypeptides. (B) Total cell lysates from U373_{RTAΔ} and U373_{RTA-E177D} cells knocked-down for SEL1L or over-expressing derlin-1-gfp, untreated or treated with proteasome inhibitor, were subjected to immunoblot analysis for RTA (lanes 1-12), SEL1L (lanes 13-24), GFP (lanes 25-36), and GAPDH (lanes 37-48). The respective polypeptides and molecular weight markers are indicated.

(Figure 6B, lanes 37-48). These results imply that ricin can utilize specific components of ER quality control machinery to be dislocated across the ER membrane.

Generation of ricin A chain chimeras.

We plan to utilize the instability of ricin A chain as the basis for a high-throughput screening to identify compounds that block ricin transport to the cytosol, thus stabilizing the ricin protein. We have been generating numerous ricin chimeras to be utilized in a cell-based high throughput screen. The chimeras include the hemagglutinin (HA) epitope tag or green fluorescence protein (GFP) and the ricin A chain. These molecules will be transduced into cells and the cells that provide the highest signal to

background values will be utilized in the proposed high-throughput screen. Figure 7 demonstrates the constructs that have been created and which constructs have been stably introduced into cells. We expect that cells that express the GFP chimeras would likely be the most robust and efficient system to perform a high-throughput screen.



Optimization of high-content screen.

Human U373 cell line that express catalytically attenuated ricin A chains fused to green fluorescence protein (GFP) (RTA-GFP) were generated. Preliminary

Figure 7. Ricin chimeras. Ricin toxin A chain (RTA) that contain either an amino- or carboxy-terminal hemagglutinin (HA) epitope tag or green fluorescence protein (GFP) chimeras will be utilized in a high-throughput screen. The constructs that have been generated or transduced in cells are designated with a (+) sign.

data using immunoblot analysis demonstrated that protein levels of RTA-GFP were unstable and were stabilized by the inclusion of

proteasome inhibitor. We proceeded to establish conditions for a high-content screen using proteasome inhibition to observe an increase in GFP fluorescent signal upon the stabilization of RTA-GFP. The quality of the assay for screening will be expressed in terms of the statistical parameter, Z' ($Z' = 1 - [3s_{C+} + 3s_{C-}] / [m_{C+} - m_{C-}]$). Where $s_{C+} + 3s_{C-}$ are the standard deviations of the positive and negative control data sets and the $m_{C+} - m_{C-}$ are the mean values of the positive and negative controls. The Z' value can predict assay fitness as excellent ($Z'=1$), good ($Z'=0.7-0.9$), or adequate ($Z'=0.5-0.7$). Only after the highest Z' score that is greater than 0.5 is achieved would the specific cell lines and conditions be utilized in a high content screen.

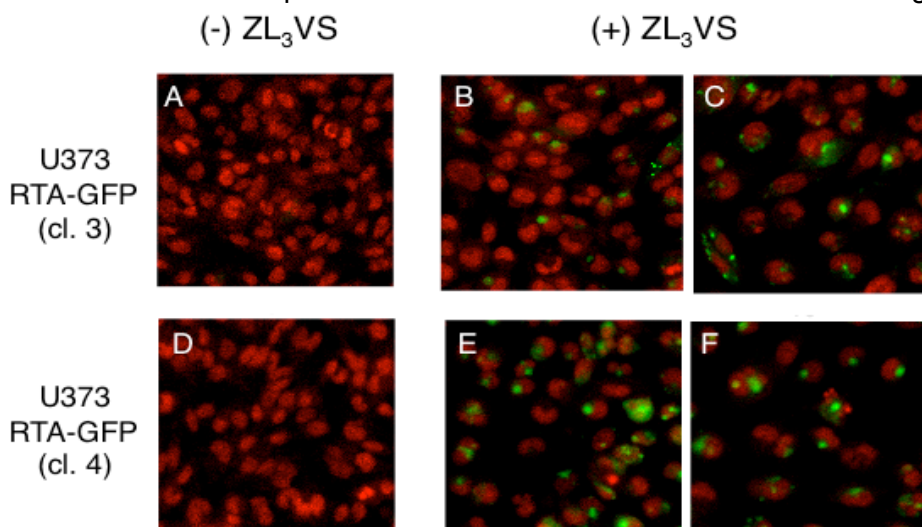


Figure 8. Visualization of stabilized RTA-GFP upon proteasome inhibition. U373_{RTA-GFP} (cl. 3) (Panels A-C) and U373_{RTA-GFP} (cl. 4) (Panels D-F) cells untreated (Panels A and D) or treated (Panels B, C, E, and F) with ZL₃VS were subjected to fluorescence microscopy. The nucleus (red) are visualized by the Hoechst stain. Stabilized RTA-GFP (green) molecules are localized to the perinuclear region.

In our initial experiment, U373_{RTA-GFP} (cl. 3) and U373_{RTA-GFP} (cl. 4) cells were untreated or treated with 2.5 μ M proteasome-specific inhibitor carboxybenzyl-leucyl-leucyl-leucine vinyl sulfone (ZL₃VS) for 14 hours. The cells were fixed with 4% paraformaldehyde, incubated with Hoechst stain (25 mg/ml) and subjected to fluorescent microscopy using the Molecular Devices ImageXpress Ultra (IXU) plate-scanning confocal microscope designed for high-throughput analysis (Figure 8, unpublished

data). The data demonstrates that the addition of ZL₃VS caused an increase in GFP signal clustered in a perinuclear region in both RTA-GFP expressing cells (Figure 8,

panels B, C, E, and F) compared to untreated cells (Figure 8, panels A and D). We observed a consistent increase in GFP clustering for U373_{RTA-GFP} cells (cl. 4). We further determined that 4,000 cells/well in a 384 well plate and ZL₃VS treatment (2.5 μ M) between 12-14 hours caused for the largest GFP fluorescent signal over background. The clustering of GFP signal allowed for the quantification of the RTA-GFP molecule into a granularity intensity and these values were used to calculate a Z' score of 0.72. Given the great Z' score, we plan to proceed with screening chemical libraries using U373_{RTA-GFP} (cl. 4) for compounds that stabilize RTA-GFP.

The facilities at the Experimental Therapeutics Institute (ETI) of MSSM will be used for the initial screen. The ETI will provide access to >114,000 small molecules, advanced high-throughput technology, technical expertise, informatics, and medicinal chemistry. The compound library includes S1 (Small Library, 12,480 compounds from Alfa-aesar, Sigma-Aldrich, and Chembridge), L1 (Large Library, 100,000 compounds from CNS, DiverSet and MicroFormat collections of Chembridge, and FDA library (2,080 compounds). They have a full-time screening staff who will assist in running the screens, and an informatics group who will assist in comparing the results of the screen. Potential hits will be evaluated for toxicity and confirmed by secondary screens. These compounds will then be utilized in cell-based ricin intoxication studies and eventual animal studies.

KEY RESEARCH ACCOMPLISHMENTS:

- Generation of ricin A toxin mutants.
- Expression of ricin A chain in human cells.
- Generation of human cells that stably express ricin A chain mutants.
- Discovery that ricin A chain is extracted through the ER membrane with fast kinetics.
- Ricin toxin A chain integrates into the membrane bilayer during the dislocation reaction.
- Ricin toxin A chain selectively utilizes cellular proteins for extraction through the ER membrane.
- Generation of a green fluorescent protein ricin A chain chimera.
- Human cells that stably express the green fluorescent protein ricin A chain chimera.
- Conditions were optimized to utilize the cells that express green fluorescent protein ricin A chain chimera in a high-content screen for the discovery of ricin inhibitors.

REPORTABLE OUTCOMES:

Manuscript:

Dislocation of ricin toxin a chains in human cells utilizes selective cellular factors. Redmann V, Oresic K, Tortorella LL, Cook JP, Lord M, Tortorella D., *J Biol Chem*. 2011 Jun 17;286(24):21231-8.

DNA constructs:

- 1) FL-RTA_{WT}, full length wild type ricin toxin A chain
- 2) FL-RTA_{E177D}, full length ricin toxin A chain with glutamic acid (E) residue 177 changed to aspartic acid (D)
- 3) FL-RTA_{Δ177-181} (RTA_Δ) full length ricin toxin A chain with a deletion of residues 177-EAARF-181
- 4) RTA_{WT}, amino terminal murine MHC class I heavy chain H2-K^b signal peptide (K^b) followed by the hemagglutinin (HA) epitope tag (AYPYDVPDYA), linker region (15 aa) and ricin A chain residues
- 5) RTA_{E177D}, Kb-HA-linker-RTA glutamic acid (E) residue 177 changed to aspartic acid (D)
- 6) RTA_Δ, Kb-HA-linker-RTA with a deletion of residues 177-EAARF-181
- 7) RTA_{E177D}-GFP, RTA_{E177D} followed by a green fluorescent protein (GFP)
- 8) RTA_Δ-GFP, RTA_Δ followed by a green fluorescent protein (GFP)

Cell lines:

- 1) U373_{RTA-E177D}
- 2) U373_{RTA_Δ}
- 3) HEK-293_{RTA-E177D}
- 4) HEK-293_{RTA_Δ}
- 5) U373_{RTA-E177D-GFP}
- 6) U373_{RTA-Δ-GFP}

CONCLUSION:

We have established human cells that express an enzymatic mutant of ricin A chain in the ER lumen to characterize ricin dislocation. Our data demonstrate that the fast kinetics of ricin A instability will be essential for creating a robust high-throughput screen. In addition, the established experiments will be used in secondary assays to validate the potential identified compounds and discover the possible protein targets. In general, we have been successful in establishing conditions to study ricin toxin transport across the ER membrane and have validated the human cells to be utilized in a high-throughput screen to discover ricin toxin transport/dislocation inhibitors.

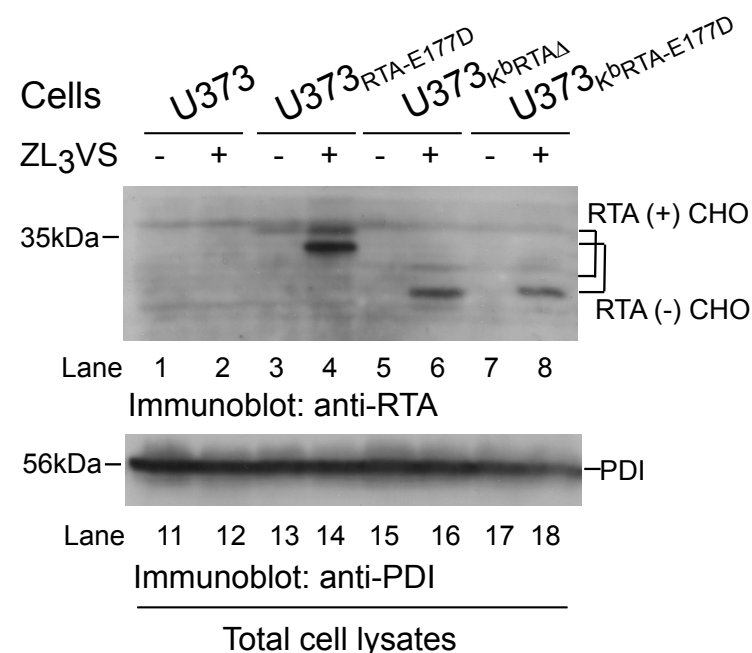
REFERENCES:

1. J. M. Lord, L. M. Roberts, J. D. Robertus, *Faseb J* 8, 201 (Feb, 1994).
2. S. M. Lehar *et al.*, *Protein Eng* 7, 1261 (Oct, 1994).
3. R. A. Spooner, D. C. Smith, A. J. Easton, L. M. Roberts, J. M. Lord, *Virology* 3, 26 (2006).
4. B. Hazes, R. J. Read, *Biochemistry* 36, 11051 (1997).
5. S. S. Vembar, J. L. Brodsky, *Nat Rev Mol Cell Biol* 9, 944 (Dec, 2008).
6. M. S. Lewis, R. J. Youle, *J Biol Chem* 261, 11571 (Sep 5, 1986).

7. R. A. Spooner *et al.*, *Biochem J* 383, 285 (Oct 15, 2004).
8. P. J. Day *et al.*, *J Biol Chem* 276, 7202 (2001).
9. N. Hosokawa *et al.*, *EMBO Rep* 2, 415 (May, 2001).
10. M. Slominska-Wojewodzka, T. F. Gregers, S. Walchli, K. Sandvig, *Mol Biol Cell* 17, 1664 (Apr, 2006).
11. J. Wesche, A. Rapak, S. Olsnes, *J Biol Chem* 274, 34443 (1999).
12. R. A. Spooner *et al.*, *Proc Natl Acad Sci U S A* 105, 17408 (Nov 11, 2008).
13. K. Eiklid, S. Olsnes, A. Pihl, *Exp Cell Res* 126, 321 (Apr, 1980).
14. S. Olsnes, C. Fernandez-Puentes, L. Carrasco, D. Vazquez, *European Journal of Biochemistry* 60, 281 (1975).
15. R. S. Marshall *et al.*, *J Biol Chem* 283, 15869 (Jun 6, 2008).
16. X. P. Li, M. Baricevic, H. Saidasan, N. E. Tumer, *Infect Immun* 75, 417 (Jan, 2007).
17. J. C. Simpson *et al.*, *FEBS Lett* 459, 80 (1999).
18. A. Frankel *et al.*, *Mol Cell Biol* 9, 415 (Feb, 1989).
19. D. Schlossman *et al.*, *Mol Cell Biol* 9, 5012 (Nov, 1989).
20. S. C. Allen *et al.*, *FEBS J* 274, 5586 (Nov, 2007).
21. F. Maley, R. B. Trimble, A. L. Tarentino, T. H. Plummer, Jr., *Anal Biochem* 180, 195 (Aug 1, 1989).
22. S. Li *et al.*, *Mol Biol Cell* 21, 2543 (Aug 1, 2010).
23. A. Di Cola, L. Frigerio, J. M. Lord, A. Ceriotti, L. M. Roberts, *Proc Natl Acad Sci U S A* 98, 14726 (2001).
24. A. Di Cola, L. Frigerio, J. M. Lord, L. M. Roberts, A. Ceriotti, *Plant Physiol* 137, 287 (Jan, 2005).
25. E. J. Wiertz *et al.*, *Cell* 84, 769 (1996b).
26. B. M. Baker, D. Tortorella, *J Biol Chem* 282, 26845 (Sep 14, 2007).
27. S. Patel, M. Latterich, *Trends Cell Biol* 8, 65 (Feb, 1998).
28. E. Fiebigel *et al.*, *Mol Biol Cell* 15, 1635 (Apr, 2004).
29. B. Mueller, E. J. Klemm, E. Spooner, J. H. Claessen, H. L. Ploegh, *Proc Natl Acad Sci U S A* 105, 12325 (Aug 26, 2008).
30. B. Mueller, B. N. Lilley, H. L. Ploegh, *J Cell Biol* 175, 261 (Oct 23, 2006).
31. B. N. Lilley, H. L. Ploegh, *Nature* 429, 834 (Jun 24, 2004).
32. F. Sun *et al.*, *J. Biol. Chem.* 281, 36856 (December 1, 2006, 2006).
33. Y. Ye, Y. Shibata, C. Yun, D. Ron, T. A. Rapoport, *Nature* 429, 841 (Jun 24, 2004).

APPENDICES

SUPPORTING DATA:



Supporting Data Figure 1: RTA mutants lacking an N-terminal epitope tag accumulates as deglycosylated intermediate. U373 cells that stably express K^bHA-RTA^{E177D} (U373^{RTA-E177D}), K^b-RTA_Δ (U373^{KbRTAΔ}), or K^b-RTA^{E177D} (U373^{KbRTA-E177D}) were treated with or without proteasome inhibitor ZL₃VS to examine the accumulation of RTA polypeptides. The accumulation of both glycosylated ((+) CHO) and deglycosylated ((-) CHO) forms of RTA molecules in all of the constructs is indicated (lanes 4, 6, and 8). The respective polypeptides and molecular weight markers are indicated.

Dislocation of Ricin Toxin A Chains in Human Cells Utilizes Selective Cellular Factors^{*S}

Received for publication, March 1, 2011, and in revised form, April 19, 2011 Published, JBC Papers in Press, April 28, 2011, DOI 10.1074/jbc.M111.234708

Veronika Redmann^{‡1,2}, Kristina Oresic^{‡1}, Lori L. Tortorella^{‡3}, Jonathan P. Cook[§], Michael Lord[§], and Domenico Tortorella^{‡4}

From the [‡]Department of Microbiology, Mount Sinai School of Medicine, New York, New York 10029 and the [§]Department of Biological Sciences, University of Warwick, Coventry CV4 7AL, United Kingdom

Ricin is a potent A-B toxin that is transported from the cell surface to the cytosol, where it inactivates ribosomes, leading to cell death. Ricin enters cells via endocytosis, where only a minute number of ricin molecules reach the endoplasmic reticulum (ER) lumen. Subsequently, the ricin A chain traverses the ER bilayer by a process referred to as dislocation or retrograde translocation to gain access to the cytosol. To study the molecular processes of ricin A chain dislocation, we have established, for the first time, a human cell system in which enzymatically attenuated ricin toxin A chains (RTA_{E177D} and RTA_{Δ177–181}) are expressed in the cell and directed to the ER. Using this human cell-based system, we found that ricin A chains underwent a rapid dislocation event that was quite distinct from the dislocation of a canonical ER soluble misfolded protein, null Hong Kong variant of α_1 -antitrypsin. Remarkably, ricin A chain dislocation occurred via a membrane-integrated intermediate and utilized the ER protein SEL1L for transport across the ER bilayer to inhibit protein synthesis. The data support a model in which ricin A chain dislocation occurs via a novel strategy of utilizing the hydrophobic nature of the ER membrane and selective ER components to gain access to the cytosol.

Ricin toxin is a toxic polypeptide found in castor beans (*Ricinus communis*) (1) comprised of a catalytically active polypeptide (A chain or RTA)⁵ covalently linked by a disulfide bond to a lectin-binding B subunit (B chain). Like most A-B toxins, the specificity of the B chains for cell surface receptors dictates cell entry. In the case of ricin toxin, the galactose-specific lectin-binding domain of the B chain interacts with cell surface glyco-

lipids and glycoproteins, allowing the toxin to enter the cell via clathrin-dependent and clathrin-independent endocytosis (2).

Following endocytosis, ricin toxin is transported in a retrograde manner through the Golgi and ER and into the cytosol by a similar manner as Shiga toxin, cholera toxin, *Pseudomonas* exotoxin A, and pertussis toxin (3). These toxins are proposed to utilize protein kinases during the endocytosis step (4). In contrast, other A-B toxins such as diphtheria toxin and anthrax toxin enter the cytoplasm following a low pH-induced translocation event directly from endocytic vesicles (3).

The retrograde trafficking of ER-directed toxins requires numerous cellular factors to reach the ER lumen (4). Both ricin and Shiga toxin are dependent on Vps34, a PI3K, and members of the sorting nexin family of proteins. In the case of ricin toxin, it is independent of Rab-9 and Rab-11 (5) and dependent on dynamin (6) and cellular cholesterol levels (7). A recent high-throughput screen identified small molecule inhibitors that demonstrate the ability to protect cells from ricin toxicity by targeting endosome-to-Golgi retrieval factors, specifically syntaxins 5 and 6 (8).

Despite the lack of a KDEL sequence, the heterodimer is transported from the Golgi apparatus to the ER lumen. While in the ER, the ricin A chain disassociates from the ricin toxin B chain and is transported across the membrane by a process referred to as dislocation or retrograde translocation (9). Once in the cytosol, the A chain acts as an N-glycosidase, which inactivates the ribosome and eventually causes cell death. However, ricin-induced cell death may also be due to inhibition of processes other than translation shutdown (10).

Ricin takes advantage of the ER quality control machinery, a cell system that normally scrutinizes nascent polypeptides and disposes of misfolded proteins by proteasome destruction (11). The ER chaperones PDI and calreticulin are proposed to play a role in ricin transport across the ER membrane (12, 13). In addition, EDEM1 (ER degradation-enhancing α -mannosidase I-like protein 1), which is involved in the degradation of misfolded ER proteins (14), also participates in ricin dislocation (15). Recently, ricin studies in yeast cells demonstrated that Hrd1p (HMG-CoA reductase degradation-1 protein) is implicated in ricin dislocation (16). The toxin is proposed to be extracted through the ER membrane via the Sec61 translocon (17), but a recent study suggests that the Hrd1p complex may act as the dislocon (18). Once dislocated, the Hsc70 cytosolic chaperone machinery protects the ricin A chain from Hsp90-assisted cytosolic degradation (19). The mechanism of ricin dislocation in human cells has not been well defined despite the

^{*} This work was supported, in whole or in part, by National Institutes of Health Grant AI060905. This work was also supported by Defense Threat Reduction Agency Contract W81XWH-10-2-0048 and the Irma T. Hirsch Trust.

^S The on-line version of this article (available at <http://www.jbc.org>) contains supplemental Fig. 1.

¹ Both authors contributed equally to this work.

² Predoctoral trainee supported in part by United States Public Health Service Institutional Research Training Award AI07647 and the Kadlec Medical Center Foundation.

³ Present address: Weill Cornell Medical College, New York, NY 10065.

⁴ To whom correspondence should be addressed: Dept. of Microbiology, Mount Sinai School of Medicine, One Gustave L. Levy Place, P. O. Box 1124, New York, NY 10029. Tel.: 212-241-5447; Fax: 212-241-7336; E-mail: domenico.tortorella@mssm.edu.

⁵ The abbreviations used are: RTA, ricin toxin A chain; ER, endoplasmic reticulum; PDI, protein-disulfide isomerase; Endo H, endoglycosidase H; ZL₃VS, carboxybenzyl-leucyl-leucyl-leucyl vinyl sulfone; PNGase, peptide N-glycanase; α_1 -AT_{HKnul}, null Hong Kong variant α_1 -antitrypsin.

identification of cellular factors that ricin utilizes for dislocation.

The potency of ricin to inactivate 2000 ribosomes/min precludes the need for a large number of molecules to reach the cytoplasm (20, 21). To characterize one of the rate-limiting steps of ricin entry, dislocation, a human cell system has been created, for the first time, that expresses an enzymatic mutant of the ricin A chain in the ER. Using this model system, ricin A chain dislocation occurs in a unique manner, utilizing the ER membrane itself as well as ER proteins.

EXPERIMENTAL PROCEDURES

Cell Lines and Antibodies—Human U373-MG astrocytoma-expressing RTA polypeptides (U373_{RTAΔ} and U373_{RTA-E177D}) were generated and maintained as described (22). Anti-ricin toxin, anti-GAPDH, anti- α_1 -antitrypsin, anti-SEL1L (suppressor of lin-12-like), anti- γ -tubulin, anti-GFP, and anti-p97 antibodies were purchased from Biodesign International, Millipore Corp., Chemicon International Inc., Sigma, Santa Cruz Biotechnology, and Abcam, respectively. Anti-HA (12CA5) antibodies were purified from hybridoma cells (23). The anti-calnexin monoclonal antibody (AF8) and anti-PDI antibody were gifts from Dr. Brenner (Harvard Medical School, Boston, MA) and Dr. Ploegh (Whitehead Institute, Cambridge, MA), respectively.

cDNA Constructs—Ricin toxin mutant chimeras RTA_{E177D} and RTA_{Δ177–181} (RTA_Δ) (24) were generated from PCR fragments (22) using full-length wild-type ricin toxin A chain (FL-RTA_{WT}) cDNA as a template. RTA_{E177D} represents a site-directed point mutant in which residue 177 (glutamic acid) was changed to aspartic acid. The RTA_Δ mutant is a deletion construct lacking residues ¹⁷⁷EAARF¹⁸¹. Finally, the chimeras consisted of an N-terminal murine MHC class I heavy chain H2-K^b signal peptide (K^b) followed by the HA epitope tag (AYPYDVP-DYA), linker region (15 amino acids), and RTA_{WT}, RTA_{E177D}, or RTA_Δ. The Derlin-1-GFP construct was generated as a chimera by fusing the Derlin-1 cDNA to enhanced GFP cDNA. The shRNA construct against SEL1L was a kind gift from Dr. Ploegh. SEL1L knockdown in HeLa cells was performed using shRNAs from Santa Cruz Biotechnology.

Cell Lysis, Immunoprecipitation, SDS-PAGE, and Endoglycosidase H and Peptide N-Glycanase Assays—Briefly, cells (1×10^6) were lysed in 0.5% Nonidet P-40 lysis mixture, followed by incubation with the respective antibody and protein A-agarose beads (22). The immunoprecipitates were subjected to immunoblot analysis using the respective immunoglobulin. Endoglycosidase H and peptide N-glycanase (New England Biolabs) assays were performed at 37 °C for 1.5 h (100 units of enzyme/reaction).

Pulse-Chase Analysis—Briefly, cells were labeled with [³⁵S]methionine (PerkinElmer Life Sciences) and chased in unlabeled methionine (25 mM) (22). RTA proteins were recovered from Nonidet P-40 cell lysates using anti-HA antibodies and resolved by SDS-PAGE (12.5%). The polyacrylamide gels were dried and exposed to autoradiography film. The polypeptide levels were quantified by densitometry analysis using an AlphaImager 3400 system (Alpha Innotech).

Subcellular Fractionation—RTA-expressing cells were mechanically homogenized using a 12- μ m ball-bearing homogenizer (12 passes; Isobiotec, Heidelberg, Germany) in homogenization buffer (100 mM Tris, 150 mM NaCl, 250 mM sucrose, 1.5 μ g/ml aprotinin, 1 μ M leupeptin, and 200 μ M phenylmethylsulfonyl fluoride) (25). Unbroken cells and other debris were pelleted at $15,000 \times g$ for 10 min at 4 °C, and the supernatants were untreated or treated with 4.5 M urea (final concentration) for 10 min at 4 °C. Supernatants were centrifuged at $100,000 \times g$ for 1 h at 4 °C. $100,000 \times g$ supernatants and pellets were resolved by SDS-PAGE (12.5%).

Isoelectric Focusing—The RTA precipitates were incubated with isoelectric focusing sample buffer (57% (w/v) urea, 2% (v/v) Nonidet P-40, 0.02% ampholytes (pH 3.5–10; Amersham Biosciences), and 0.025% 2-mercaptoethanol) and resolved on a 17-cm one-dimensional isoelectric focusing gel (57% (w/v) urea, 2% (v/v) Nonidet P-40, 15.5% acrylamide (30:1.6 acrylamide/bisacrylamide), 4% ampholytes (pH 5–7), 1% ampholytes (pH 3.5–10), and 0.4% ampholytes (pH 7–9)) for 14 h. After electrophoresis, the gel was soaked in 50% methanol, 1% (w/v) SDS, and 5 mM Tris-Cl (pH 8.0) for 2 h and subjected to immunoblot analysis (25).

Ricin Activity Assays—HEK-293T cells were cotransfected with RTA constructs and a GFP expression plasmid (pCAGGS-GFP) using Lipofectamine 2000 (Invitrogen). Thirty hours post-transfection, GFP-positive cells were examined using a Beckman Coulter Cytomics FC 500 flow cytometer, and the data were analyzed using FlowJo software. HeLa cell lines seeded in 96-well plates at 2×10^4 cells/well were incubated with doubling dilutions of ricin in quadruplicate for various times. The cells were incubated with ³⁵S-Pro-mix (PerkinElmer Life Sciences). The amount of radioactivity incorporated into TCA-precipitable proteins was measured by scintillation counting in a MicroBeta TriLux 1450 counter, and IC₅₀ values (representing the concentration of toxin reducing protein synthesis by 50% relative to untreated control cells) were recorded.

RESULTS

Ricin A Chains Directed to the ER Block Protein Synthesis—The investigation of ricin toxin transport across the ER membrane has been hampered by the low number of toxin molecules that reach the ER lumen when added extracellularly (17). Hence, we aimed to create a human cell-based assay to specifically study RTA transport across the ER membrane. In line with this objective, we initially confirmed that RTA molecules directed to the ER (10, 26) in human cells limited protein expression. FL-RTA_{WT} and wild-type mature RTA equipped with a murine MHC class I molecule (K^b) signal peptide and an HA epitope tag at its N terminus (RTA_{WT}) were cotransfected with a GFP expression plasmid in HEK-293T cells and evaluated for GFP fluorescence using flow cytometry (Fig. 1, A–D). The lack of GFP fluorescent cells is indicative of functionally active RTA molecules. FL-RTA_{WT} and RTA_{WT} limited the expression of GFP in a significant percentage of cells (2 and 15%, respectively) (Fig. 1, C and D) compared with cells transfected with GFP alone (85%) (Fig. 1B). These data suggest that ER-directed RTA molecules are dislocated across the ER and to the cytosol, where they inhibit protein synthesis.

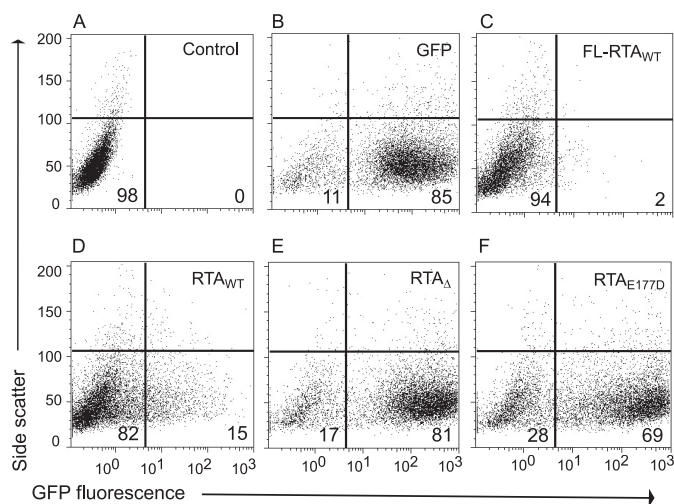


FIGURE 1. RTA inhibits protein expression in human cells. HEK-293T cells transfected with an empty plasmid (Control; A) or a GFP-expressing plasmid (B) with FL-RTA_{WT} (C), RTA_{WT} (D), RTA_Δ (E), and RTA_{E177D} (F) were analyzed for GFP expression using flow cytometry. The values in the quadrants represent percentage of total cells.

Ricin A Chain Expression in Human Cells—Because of the toxic nature of wild-type RTA, we cloned ricin A chain mutants (RTA_{E177D} and RTA_Δ; see “Experimental Procedures”) that are enzymatically attenuated to study A chain dislocation (27, 28). RTA_{E177D} is a site-directed mutant with attenuated activity that is structurally similar to wild-type RTA (29), whereas RTA_Δ has deletion of residues 177–181. Like RTA_{WT}, these constructs were also engineered with the N-terminal K^b signal peptide and HA epitope tag. An initial experiment was performed to determine whether RTA_{E177D} and RTA_Δ inhibit protein synthesis. GFP-positive cells were examined in HEK-293T cells cotransfected with RTA_{E177D} and RTA_Δ and a GFP expression plasmid (Fig. 1, E and F). The RTA_{E177D} and RTA_Δ mutants had a diminished ability to affect GFP expression (Fig. 1, E and F), with RTA_{E177D} retaining some capacity to inhibit GFP expression. These data demonstrate that ricin A chain mutants have a limited capacity to prevent protein expression.

To study RTA dislocation, human U373 cells that stably express RTA_{E177D} and RTA_Δ (see “Experimental Procedures”) (Fig. 2) were created. Our initial experiment examined the acquisition of an N-linked glycan onto RTA_{E177D} and RTA_Δ to confirm their localization to the ER. RTA_{E177D} and RTA_Δ molecules recovered from these cells were subjected to endoglycosidase H (Endo H) treatment, followed by immunoblot analysis (Fig. 2A). Endo H preferentially cleaves high mannose-containing N-linked oligosaccharides characteristic of ER-resident molecules (30). RTA_{E177D} and RTA_Δ polypeptides with the predicted molecular mass were recovered from cell lysates (Fig. 2A, lanes 3 and 5). As expected, faster migrating RTA polypeptides were observed upon treatment with Endo H (Fig. 2A, lanes 4 and 6). The difference in the relative molecular mass of the two species (~3–4 kDa) confirmed that the RTA polypeptides acquired a single N-linked glycan and were retained in the ER. These data demonstrate that this human cell-based assay can be utilized to study ricin dislocation.

Ricin A Chains Are Subjected to Proteasome Degradation—We next investigated the stability of the RTA polypeptides in

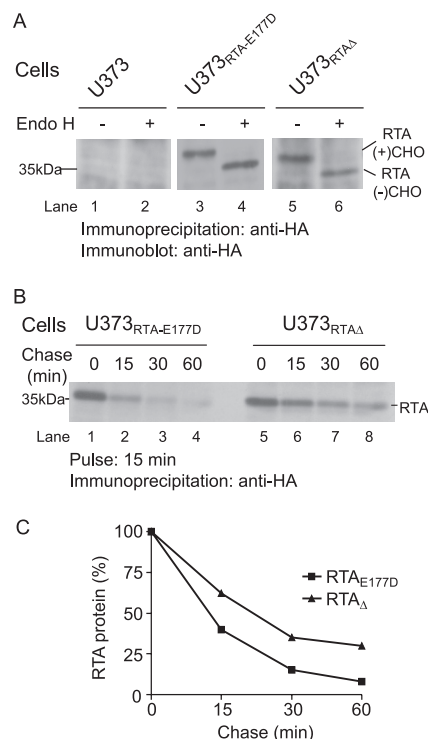


FIGURE 2. RTA polypeptides are unstable ER proteins. A, U373, U373_{RTA-E177D}, and U373_{RTAΔ} cell lysates were incubated with anti-HA antibodies. The recovered precipitates were subjected to Endo H digestion and analyzed by immunoblot analysis. RTA(+)-CHO and RTA(-)-CHO, glycosylated and deglycosylated molecules, respectively. B, U373_{RTA-E177D} and U373_{RTAΔ} cells were pulsed with [³⁵S]methionine for 15 min and chased for up to 60 min. The recovered RTA polypeptides were resolved by SDS-PAGE and detected by autoradiography. C, the levels of RTA polypeptides were quantified by densitometry and are plotted as a percentage to the 0-min chase point (100%). RTA polypeptides and molecular mass markers are indicated.

U373_{RTA-E177D} and U373_{RTAΔ} cells by pulse-chase analysis (Fig. 2, B and C). The cells were metabolically labeled with [³⁵S]methionine for 15 min and chased for up to 60 min. Strikingly, the half-life of RTA_{E177D} (<10 min) was less than that of RTA_Δ (~20 min) (Fig. 2, B, lanes 1–8, and C). Given that ricin utilizes ER quality control to gain access to the cytosol (9, 16), it is expected that a population of ricin would be degraded. However, the rapid half-life of RTA_{E177D} expressed in human cells compared with yeast cells (16, 26) and plant cells (31, 32) suggests that RTA is efficiently transported out of the ER in human cells.

Are RTA polypeptides targeted for proteasome-dependent degradation? To address this question, U373_{RTA-E177D} and U373_{RTAΔ} cells treated with or without the proteasome inhibitor carboxybenzyl-leucyl-leucyl-leucyl vinyl sulfone (ZL₃VS; 25 μM, 1 h) were subjected to pulse-chase analysis (Fig. 3). As expected, RTA polypeptides decreased over the chase period (Fig. 3, A and B, lanes 1–3). Strikingly, inclusion of the proteasome inhibitor stabilized both RTA_{E177D} and RTA_Δ molecules (Fig. 3, A and B, lanes 4–6). In addition, proteasome inhibition enabled the recovery of a faster migrating polypeptide intermediate during the chase, most likely deglycosylated RTA species (Fig. 3, A and B, lanes 4–6, *). Collectively, the data demonstrate that ricin A chains are eventually degraded in a proteasome-dependent manner.

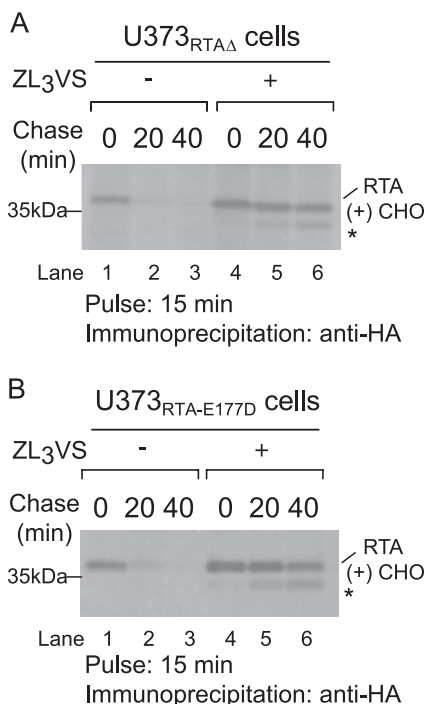


FIGURE 3. RTA polypeptides are stabilized in the presence of the proteasome inhibitor. U373_{RTAΔ} (A) and U373_{RTA-E177D} (B) cells treated with or without the proteasome inhibitor ZL₃VS were pulsed with [³⁵S]methionine for 15 min and chased for up to 40 min. RTA polypeptides were recovered with an anti-HA antibody, resolved by SDS-PAGE, and detected by autoradiography. RTA polypeptides and molecular mass markers are indicated. The asterisks indicate faster migrating species. RTA(+)/CHO, glycosylated molecules.

Characterization of RTA_{E177D} and RTA_Δ Intermediates—We next optimized conditions to observe the faster migrating RTA species. Total cell lysates from U373_{RTA-E177D} and U373_{RTAΔ} cells treated with ZL₃VS (10 μM) for up to 5 h were subjected to immunoblot analysis (Fig. 4A). Strikingly, RTA_{E177D} proteins were almost completely converted to the faster migrating species after 2 h of ZL₃VS treatment (Fig. 4A, lanes 9–12). In contrast, RTA_Δ molecules displayed a biphasic conversion in which an increase in glycosylated RTA_Δ was observed during the early times of proteasome inhibition (Fig. 4A, lanes 2 and 3), followed by an accumulation of glycosylated and faster migrating species during later times of ZL₃VS treatment (lanes 4–6). Interestingly, the ratio of glycosylated (RTA(+)/CHO) to faster migrating species following proteasome treatment significantly varied between the RTA mutants (Fig. 4A, lanes 1–6 and 7–12, respectively). These results suggest that RTA_{E177D} and RTA_Δ are likely processed differently due to the folding status of the polypeptide.

To address the N-linked glycosylation status of the RTA_Δ and RTA_{E177D} intermediates, we examined their sensitivity to *in vitro* glycosidase treatment (Fig. 4B). RTA polypeptides recovered from U373_{RTA-E177D} and U373_{RTAΔ} cells treated with the proteasome inhibitor (2.5 μM, 10 h) were undigested or digested with Endo H or peptide N-glycanase (PNGase), followed by immunoblot analysis (Fig. 4B). U373 cells were used as a negative control. As expected, two species of RTA polypeptides were observed exclusively from proteasome inhibitor-treated cells (Fig. 4B, lanes 10 and 16). Moreover, only the slower migrating glycosylated species were sensitive to Endo H

and PNGase digestion, resulting in the faster migrating form of the RTA-reactive polypeptides (Fig. 4B, lanes 11, 12, 17, and 18). Calnexin levels demonstrated equivalent protein loading (Fig. 4B, lanes 19–36). These data suggest that the faster migrating RTA species are deglycosylated intermediates generated from the dislocation of ricin polypeptides.

To confirm that the N-terminal epitope tag does not affect the processing of the RTA polypeptides, we examined the accumulation of untagged RTA mutants upon proteasome inhibition (supplemental Fig. 1). Cell lysates from proteasome inhibitor-treated U373, U373_{RTA-E177D}, U373_{KbRTAΔ}, and U373_{KbRTA-E177D} cells were subjected to immunoblot analysis. Two species of RTA molecules, glycosylated and deglycosylated, accumulated in proteasome inhibitor-treated cells, demonstrating that the stability of both forms of RTA is independent of the N-terminal epitope tag.

To confirm that the faster migrating RTA species were indeed digested by cellular PNGase, the RTA polypeptides were resolved on a one-dimensional isoelectric focusing gel. PNGase cleavage results in the conversion of asparagine to aspartic acid, causing a more acidic species, thus changing the overall charge of the polypeptide (33). RTA polypeptides recovered from U373_{RTA-E177D} cells treated with the proteasome inhibitor (2.5 μM, 10 h) were untreated or treated with Endo H or PNGase, resolved on a one-dimensional isoelectric focusing gel, and subjected to immunoblot analysis (Fig. 4C). RTA_{E177D} polypeptides from ZL₃VS-treated cells migrated as two discrete bands likely corresponding to species with different charges (Fig. 4C, lane 1, * and **). Strikingly, *in vitro* PNGase digestion of RTA_{E177D} polypeptides caused the polypeptides to migrate at a similar position as the more acidic RTA molecules (Fig. 4C, lane 2, **), whereas Endo H treatment did not alter the migration pattern of the RTA_{E177D} polypeptides (lane 3). The same result was observed for RTA_Δ.⁶ These results demonstrate that RTA polypeptides are subjected to cellular deglycosylation during dislocation.

Ricin A Chains Utilize ER Membrane Factors for Efficient Dislocation—To characterize the membrane topology of stabilized RTA polypeptides, we performed a subcellular fractionation protocol (see “Experimental Procedures”). Membrane microsomes from U373_{RTA-E177D} and U373_{RTAΔ} cells treated with the proteasome inhibitor (2.5 μM, 10 h) were incubated with 4.5 M urea and subjected to high-speed centrifugation (100,000 × g) to separate the membrane fraction from the supernatant fraction. The 100,000 × g supernatant, 100,000 × g pellet, and total cell lysates were subjected to immunoblot analysis for RTA mutants (Fig. 5, lanes 1–10) and p97 (lanes 11–20). The p97 polypeptide is a soluble cytosolic protein that associates with the ER membrane (34) and, as expected, was completely extracted from the bilayer upon treatment with urea (Fig. 5, lanes 12 and 14). As expected, some of the stabilized RTA_{E177D} and RTA_Δ molecules were found in the 100,000 × g supernatant (Fig. 5, lanes 6 and 8). Strikingly, a significant population of RTA_{E177D} and RTA_Δ was observed with the membrane fraction (Fig. 5, lanes 2 and 4), demonstrating that these

⁶ K. Oresic and D. Tortorella, unpublished data.

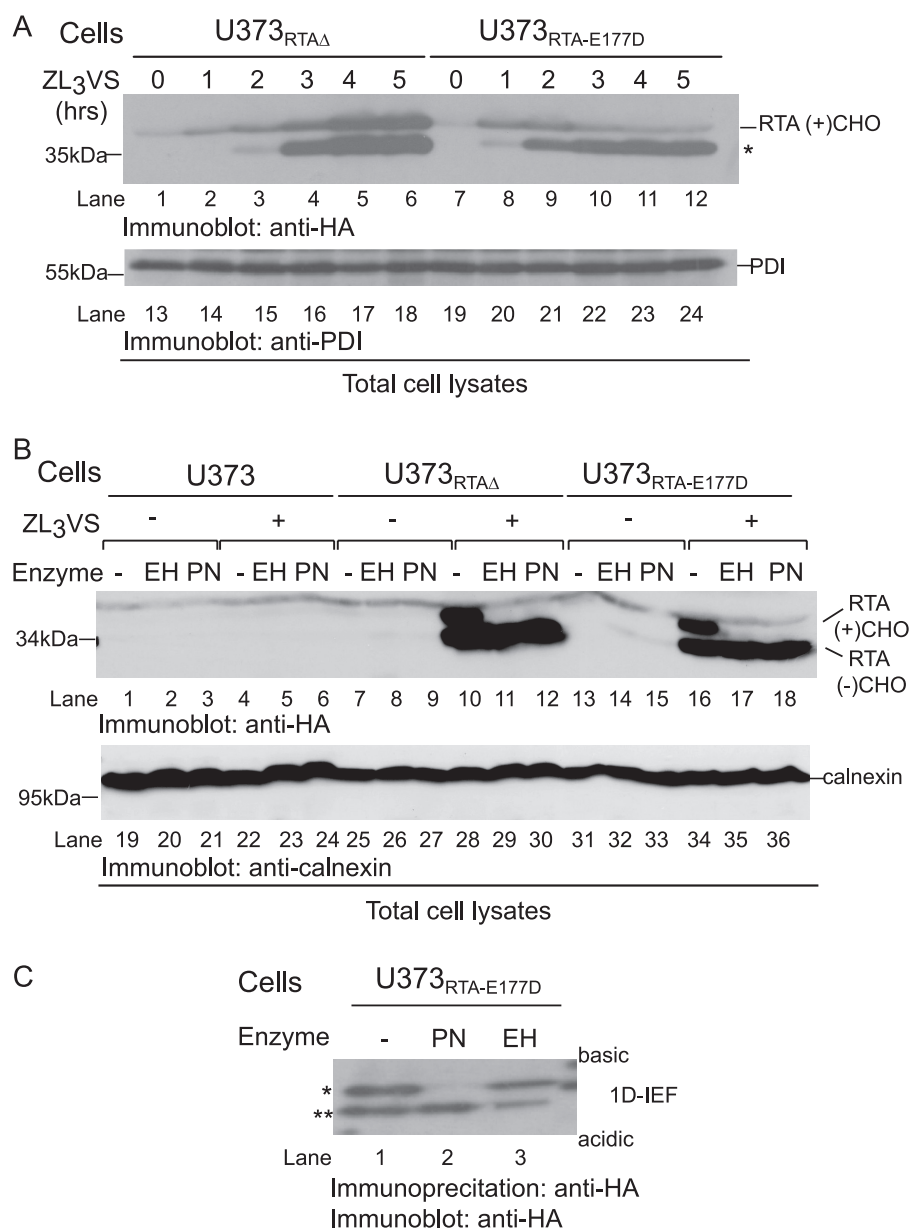


FIGURE 4. RTA molecules accumulate as deglycosylated intermediates. *A*, U373_{RTAΔ} and U373_{RTA-E177D} cells treated with ZL₃VS for up to 5 h were subjected to immunoblot analysis for RTA (lanes 1–12) and PDI (lanes 13–24). The asterisk indicates the faster migrating polypeptides. *B*, total cell lysates from U373, U373_{RTA-E177D}, and U373_{RTAΔ} cells untreated or treated with the proteasome inhibitor were subjected to Endo H (EH) or PNGase (PN). Immunoblot analysis was performed for RTA (lanes 1–18) and calnexin (lanes 19–36) proteins. RTA(+)-CHO and RTA(-)-CHO, glycosylated and deglycosylated molecules, respectively. *C*, RTA polypeptides recovered from U373_{RTA-E177D} cells treated with ZL₃VS were subjected to PNGase or Endo H treatment. Subsequently, the samples were resolved by one-dimensional isoelectric focusing (1D-IEF) and subjected to immunoblot analysis. The respective polypeptides and molecular mass markers are indicated. The asterisks (*) and (**) represent RTA molecules with different charges.

RTA molecules are integrated into the bilayer. These results imply that ricin A chains are efficiently dislocated via membrane-integrated intermediates.

Ricin A Chains Are Dislocated Utilizing Selective Components of ER Quality Control—To validate that RTA polypeptides were dislocated utilizing the ER quality control machinery, we examined the effect of a dislocation inhibitor, eeyarestatin I (35), on the stability of ricin A chains. U373_{RTA-E177D} and U373_{RTAΔ} cells treated with or without eeyarestatin I (5 μg/ml) or the proteasome inhibitor ZL₃VS (2.5 μM) were subjected to immunoblot analysis (Fig. 6A). PDI levels assured equivalent protein loading (Fig. 6A, lanes 9–16). As

expected, treatment with ZL₃VS caused a significant increase in both RTA_Δ and RTA_{E177D} polypeptides (Fig. 6A, lanes 5–8), with a difference between the levels of glycosylated (RTA(+)-CHO) and deglycosylated (RTA(-)-CHO) molecules. Interestingly, mostly glycosylated RTA_Δ and RTA_{E177D} polypeptides accumulated from cells treated with eeyarestatin I (Fig. 6A, lanes 2 and 4). However, because eeyarestatin I attenuates the process of dislocation and not proteasome function (35), it was interesting that deglycosylated forms of the ricin A chain were observed (Fig. 6A, lanes 2 and 4). Therefore, ricin A chain dislocation probably occurs using a distinct mechanism compared with ER-associated degradation substrates.

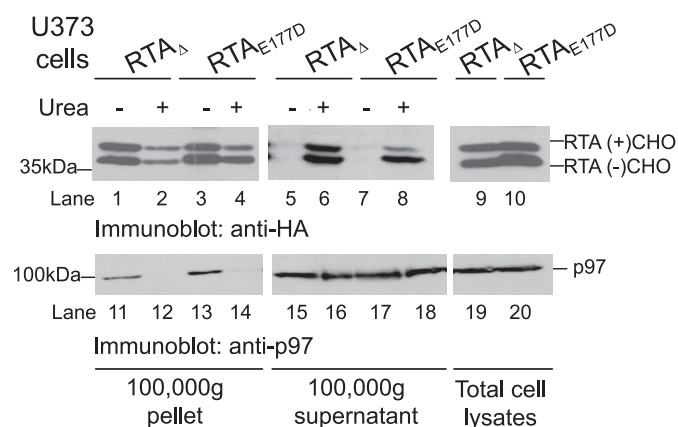


FIGURE 5. RTA dislocation utilizes membrane components. Microsomal preparations from subcellular homogenates of U373 $_{\text{RTA}\Delta}$ and U373 $_{\text{RTA}\Delta\text{E177D}}$ cells were treated with or without 4.5 M urea and centrifuged at $100,000 \times g$. Total cell lysates, $100,000 \times g$ pellets, and the $100,000 \times g$ supernatant were subjected to immunoblot analysis against RTA (lanes 1–10) and p97 (lanes 11–20). The respective polypeptides and molecular mass markers are indicated. RTA(+)*CHO* and RTA(–)*CHO*, glycosylated and deglycosylated molecules, respectively.

To further explore the involvement of dislocation-associated cellular proteins in the transport of ricin toxin across the ER membrane, we investigated the role of SEL1L and Derlin-1 in the dislocation of RTA Δ E177D and RTA Δ polypeptides. SEL1L functions as part of the mammalian HRD1 ligase complex and is proposed to be involved in the recognition of ER degradation substrates (36, 37). Derlin-1 plays a role in the extraction of certain misfolded ER proteins, and a dominant-negative form, Derlin-1-GFP, can impede substrate dislocation (38–40). U373 $_{\text{RTA}\Delta\text{E177D}}$ and U373 $_{\text{RTA}\Delta}$ cells transduced with Derlin-1-GFP and shRNA against SEL1L were untreated or treated with ZL₃VS (2.5 μM , 10 h) and subjected to immunoblot analysis (Fig. 6B). The expression of the constructs was confirmed by anti-SEL1L (Fig. 6B, lanes 13–24) and anti-GFP (lanes 25–36) immunoblotting. Derlin-1-GFP expression did not alter the levels of RTA polypeptides regardless of proteasome inhibition (Fig. 6B, lanes 1, 2, 4, 5, 7, 8, 10, and 11). These results are consistent with published findings implying that ricin toxin transport across the ER membrane is Derlin-1-independent (15). On the other hand, silencing of SEL1L resulted in a substantial increase in RTA polypeptides in both the presence and absence of proteasome inhibition (Fig. 6B, lanes 3, 6, 9, and 12). Anti-GAPDH immunoblotting indicated equal protein loading (Fig. 6B, lanes 37–48). These results imply that ricin can utilize specific components of ER quality control machinery to be dislocated across the ER membrane.

We next examined whether deficiency in SEL1L levels affects ricin toxicity (Fig. 7). Ricin holotoxin was exogenously administered to HeLa cells stably expressing shRNA against SEL1L or a control shRNA (Fig. 7A). A control cell line (C1), a cell line revealing no SEL1L knockdown (120% of the control; S8), and a cell line showing 53% knockdown (S24) were utilized in subsequent cytotoxicity experiments (Fig. 7A). After inclusion of ricin holotoxin, the incorporation of radiolabeled amino acids into nascent polypeptides was measured by scintillation counting. Protection from toxin challenge would be demonstrated if the IC₅₀ ratio of SEL1L knockdown cells to control cells is >1 .

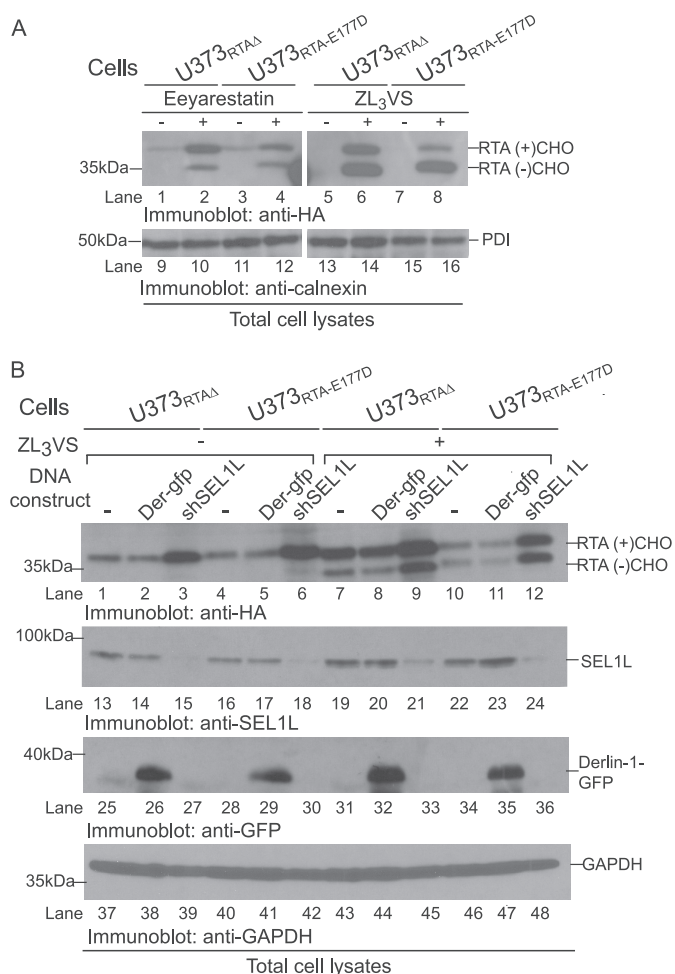


FIGURE 6. RTA is dislocated utilizing selective ER proteins. A, U373 $_{\text{RTA}\Delta}$ and U373 $_{\text{RTA}\Delta\text{E177D}}$ cells untreated or treated with eeyarestatin I and ZL₃VS were subjected to immunoblot analysis for RTA (lanes 1–8) and PDI (lanes 9–16) polypeptides. B, total cell lysates from U373 $_{\text{RTA}\Delta}$ and U373 $_{\text{RTA}\Delta\text{E177D}}$ cells knocked down for SEL1L or overexpressing Derlin-1-GFP, untreated or treated with proteasome inhibitor (ZL₃VS), were subjected to immunoblot analysis for RTA (lanes 1–12), SEL1L (lanes 13–24), GFP (lanes 25–36), and GAPDH (lanes 37–48). The respective polypeptides and molecular mass markers are indicated. RTA(+)*CHO* and RTA(–)*CHO*, glycosylated and deglycosylated molecules, respectively; Der-gfp, Derlin-1-GFP; shSEL1L, SEL1L shRNA.

The ricin IC₅₀ for S8 cells was equivalent to that for the C1 cell line (Fig. 7B). In contrast, a significant protection from ricin was observed in the SEL1L knockdown cell line (S24), ranging from 1.6- to 1.4-fold during the time course of ricin challenge (Fig. 7C). Collectively, the results indicate that ricin requires SEL1L for the dislocation of its A chain from the ER to the cytosol and subsequently induces toxicity.

The Ricin A Chain Is Not Dislocated as a Canonical Soluble Misfolded ER Protein—We compared the degradation intermediates of RTA and a canonical soluble ER degradation substrate, null Hong Kong variant of α_1 -antitrypsin (α_1 -AT $_{\text{HKnull}}$) (41, 42). The total cell lysates of U373, U373 $_{\text{RTA}\Delta\text{E177D}}$, and U373 $_{\text{RTA}\Delta}$ cells and U373 cells that stably express the α_1 -AT $_{\text{HKnull}}$ variant (U373 $_{\alpha_1\text{-AT-HKnull}}$) were untreated or treated with ZL₃VS (2.5 μM , 10 h) and subjected to immunoblot analysis (Fig. 8). PDI levels confirmed equal protein loading (Fig. 8, lanes 17–24). As expected, both glycosylated and deglycosylated RTA Δ E177D and RTA Δ molecules accumulated upon inclu-

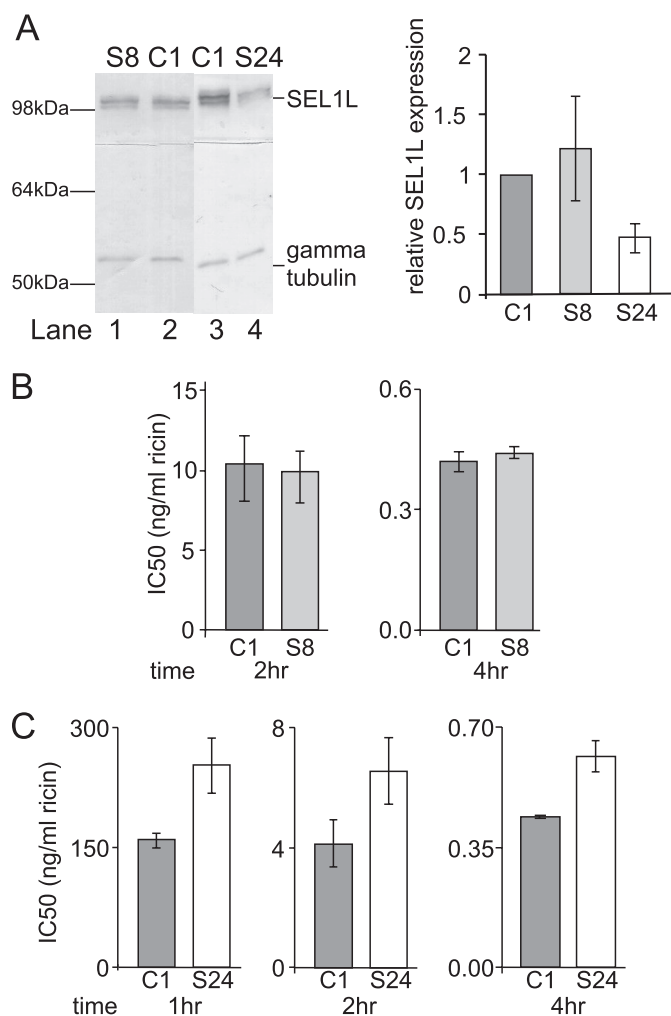


FIGURE 7. SEL1L knockdown protects cells from ricin. HeLa cells were transfected with shRNA targeted against SEL1L and a control shRNA. **A**, SEL1L levels from lysates of cells expressing a control shRNA (C1) or shRNAs targeting SEL1L (S8 and S24) were analyzed by immunoblot analysis. SEL1L and γ -tubulin were quantified to assess levels of SEL1L knockdown ($n = 8$). **B** and **C**, the cytotoxicity of ricin against the stable cell lines was measured, and the mean IC₅₀ values for different times of toxin incubation are plotted (nanograms/ml; $n = 2$). The respective polypeptides and molecular mass markers are indicated.

sion of the proteasome inhibitor (Fig. 8, lanes 4 and 6). In sharp contrast, only an increase in glycosylated α_1 -AT_{HKnull} species was observed in ZL₃VS-treated cells (Fig. 8, lane 16). These results indicate that even though both RTA and α_1 -AT_{HKnull} polypeptides represent soluble substrates of dislocation, RTA extraction across the ER membrane probably occurs in a directed manner to increase the likelihood of gaining access to the cytosol.

DISCUSSION

Ricin toxin co-opts the trafficking machinery and ER quality control to gain access to the cytosol. In this study, we established a human cell-based assay to study ricin dislocation by generating, for the first time, human cells that stably express enzymatic RTA mutants in the ER (Fig. 2). Using this human cell-based system, we demonstrated that ricin A chains are rapidly extracted from the ER in a directed manner utilizing specific ER factors to enhance their dislocation efficiency. These

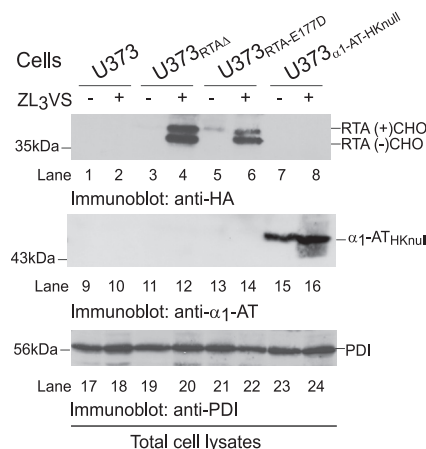


FIGURE 8. RTA is not degraded as a canonical misfolded ER protein. Total cell lysates from U373, U373_{RTAΔ}, U373_{RTA-E177D}, and U373_{α1-AT-HKnull} cells treated with ZL₃VS were subjected to immunoblot analysis for RTA (lanes 1–8), α_1 -AT_{HKnull} (lanes 9–16), and PDI (lanes 17–24). The respective polypeptides and molecular mass markers are indicated. RTA (+)CHO and RTA (-)CHO, glycosylated and deglycosylated molecules, respectively.

ER factors include the ER membrane itself (Fig. 5) and SEL1L, a component associated with the degradation of ER proteins (Figs. 6 and 7). These data support a model in which RTA is transported out of the ER by a novel strategy of co-opting specific ER proteins and the ER bilayer to gain access to the cytosol.

Ricin toxin has evolved to selectively utilize cellular proteins to promote its dislocation across the membrane bilayer. The toxin likely undergoes a conformational change induced by the interaction with ER chaperones such as calreticulin and PDI (12, 13), thus allowing its engagement with specific factors of the dislocation apparatus, SEL1L (Figs. 6 and 7) and probably Hrd1p (16); yet this process seems to act independently of Derlin-1 (Fig. 6) (15), which is unlike cholera toxin, whose dependence on Derlin-1 for dislocation remains in question (43). SEL1L is an auxiliary protein for the E3 ubiquitin ligase HRD1 (37), and the dependence of RTA dislocation on SEL1L would typically suggest that RTA is ubiquitinated prior to dislocation. Despite the low number of lysines within ricin as observed for other toxins (44), ubiquitin conjugation to ricin A chains would be selective for the purposes of dislocation (3, 45). Therefore, ricin can utilize SEL1L for dislocation, and yet a population of the A chains can escape degradation to block protein synthesis (Fig. 1).

Once targeted for extraction out of the ER, we propose that ricin A chains utilize the hydrophobic nature of the bilayer to catalyze their dislocation (Fig. 5). The recovery of membrane-integrated glycosylated A chains suggests that RTA is inserted into the bilayer due to a conformational change induced by its engagement with ER factors. In fact, the association of RTA molecules with ER microsomes upon an increase in temperature suggests that extrinsic factors can induce a partial conformational change in ricin A chains (46). The ability of ricin to insert into the bilayer would afford ricin dislocation to be less dependent on cellular proteins. Yeast cell studies demonstrate that wild-type RTA dislocation is independent of the p97-Npl4p-Ufd1p complex (16). Therefore, membrane integration of RTA may provide some of the driving force for extraction out of the ER. Alternatively, ricin A chains may be extracted from

the ER as a protein/lipid micelle (47). In either case, RTA has evolved a unique strategy to efficiently cross the ER bilayer.

The ricin A chain contains only two lysines as a possible strategy to limit ubiquitin-dependent degradation (45). Despite the low lysine number and the use of the protective nature of Hsc70, a population of ricin A chains is degraded by the proteasome (Figs. 2–4) (26). However, there are distinct differences between ricin A chains and misfolded ER proteins that demonstrate that ricin co-opts select components of ER quality control to gain access to the cytosol. A major difference is observed in the dislocation kinetics of ricin as evaluated by the stability of glycosylated proteins and the accumulation of deglycosylated intermediates. This is apparent when compared with the levels of the canonical soluble misfolded ER-associated degradation substrate α_1 -AT_{HKnull} in proteasome inhibitor-treated cells (Fig. 8). Another factor may be the ability of ricin to integrate into the bilayer. Membrane integration may allow limited exposure to the degradation machinery and permit RTA to escape destruction for a period of time to inhibit protein synthesis (Fig. 1). Thus, the ricin has evolved strategies inherent to its sequence and structure to bypass ER-associated degradation to reach the cytosol and inhibit protein synthesis.

Our human cell-based ricin dislocation assay is a powerful system to elucidate the molecular details of how ricin co-opts ER quality control, bypassing the ubiquitin-proteasome degradation process and gaining access to the cytosol. Our future objectives will be focused on delineating the components of the ER that ricin toxin co-opts to gain access to the cytosol.

Acknowledgment—We thank Dr. Matthew Bogyo (Stanford University) for the generous gift of the proteasome inhibitor.

REFERENCES

- Lord, J. M., Roberts, L. M., and Robertus, J. D. (1994) *FASEB J.* **8**, 201–208
- Lehar, S. M., Pedersen, J. T., Kamath, R. S., Swimmer, C., Goldmacher, V. S., Lambert, J. M., Blättler, W. A., and Guild, B. C. (1994) *Protein Eng.* **7**, 1261–1266
- Hazes, B., and Read, R. J. (1997) *Biochemistry* **36**, 11051–11054
- Sandvig, K., Torgersen, M. L., Engedal, N., Skotland, T., and Iversen, T. G. (2010) *FEBS Lett.* **584**, 2626–2634
- Iversen, T. G., Skretting, G., Llorente, A., Nicoziani, P., van Deurs, B., and Sandvig, K. (2001) *Mol. Biol. Cell* **12**, 2099–2107
- Llorente, A., Rapak, A., Schmid, S. L., van Deurs, B., and Sandvig, K. (1998) *J. Cell Biol.* **140**, 553–563
- Grimmer, S., Iversen, T. G., van Deurs, B., and Sandvig, K. (2000) *Mol. Biol. Cell* **11**, 4205–4216
- Stechmann, B., Bai, S. K., Gobbo, E., Lopez, R., Merer, G., Pinchard, S., Panigai, L., Tenza, D., Raposo, G., Beaumelle, B., Sauvage, D., Gillet, D., Johannes, L., and Barbier, J. (2010) *Cell* **141**, 231–242
- Spooner, R. A., Smith, D. C., Easton, A. J., Roberts, L. M., and Lord, J. M. (2006) *Virology* **3**, 26
- Li, X. P., Baricevic, M., Saidasan, H., and Tumer, N. E. (2007) *Infect. Immun.* **75**, 417–428
- Vembar, S. S., and Brodsky, J. L. (2008) *Nat. Rev. Mol. Cell Biol.* **9**, 944–957
- Day, P. J., Owens, S. R., Wesche, J., Olsnes, S., Roberts, L. M., and Lord, J. M. (2001) *J. Biol. Chem.* **276**, 7202–7208
- Spooner, R. A., Watson, P. D., Marsden, C. J., Smith, D. C., Moore, K. A., Cook, J. P., Lord, J. M., and Roberts, L. M. (2004) *Biochem. J.* **383**, 285–293
- Hosokawa, N., Wada, I., Hasegawa, K., Yoriyuzi, T., Tremblay, L. O., Herscovics, A., and Nagata, K. (2001) *EMBO Rep.* **2**, 415–422
- Slominska-Wojewodzka, M., Gregers, T. F., Wälchli, S., and Sandvig, K. (2006) *Mol. Biol. Cell* **17**, 1664–1675
- Li, S., Spooner, R. A., Allen, S. C., Guise, C. P., Ladds, G., Schnöder, T., Schmitt, M. J., Lord, J. M., and Roberts, L. M. (2010) *Mol. Biol. Cell* **21**, 2543–2554
- Wesche, J., Rapak, A., and Olsnes, S. (1999) *J. Biol. Chem.* **274**, 34443–34449
- Carvalho, P., Stanley, A. M., and Rapoport, T. A. (2010) *Cell* **143**, 579–591
- Spooner, R. A., Hart, P. J., Cook, J. P., Pietroni, P., Rogon, C., Höfeld, J., Roberts, L. M., and Lord, J. M. (2008) *Proc. Natl. Acad. Sci. U.S.A.* **105**, 17408–17413
- Eiklid, K., Olsnes, S., and Pihl, A. (1980) *Exp. Cell Res.* **126**, 321–326
- Olsnes, S., Fernandez-Puentes, C., Carrasco, L., and Vazquez, D. (1975) *Eur. J. Biochem.* **60**, 281–288
- Oresic, K., Noriega, V., Andrews, L., and Tortorella, D. (2006) *J. Biol. Chem.* **281**, 19395–19406
- Harlow, E., Fianza, B. R., Jr., and Schley, C. (1985) *J. Virol.* **55**, 533–546
- Chaddock, J. A., and Roberts, L. M. (1993) *Protein Eng.* **6**, 425–431
- Baker, B. M., and Tortorella, D. (2007) *J. Biol. Chem.* **282**, 26845–26856
- Simpson, J. C., Roberts, L. M., Römisch, K., Davey, J., Wolf, D. H., and Lord, J. M. (1999) *FEBS Lett.* **459**, 80–84
- Frankel, A., Schlossman, D., Welsh, P., Hertler, A., Withers, D., and Johnston, S. (1989) *Mol. Cell. Biol.* **9**, 415–420
- Schlossman, D., Withers, D., Welsh, P., Alexander, A., Robertus, J., and Frankel, A. (1989) *Mol. Cell. Biol.* **9**, 5012–5021
- Allen, S. C., Moore, K. A., Marsden, C. J., Fülöp, V., Moffat, K. G., Lord, J. M., Ladds, G., and Roberts, L. M. (2007) *FEBS J.* **274**, 5586–5599
- Maley, F., Trimble, R. B., Tarentino, A. L., and Plummer, T. H., Jr. (1989) *Anal. Biochem.* **180**, 195–204
- Di Cola, A., Frigerio, L., Lord, J. M., Ceriotti, A., and Roberts, L. M. (2001) *Proc. Natl. Acad. Sci. U.S.A.* **98**, 14726–14731
- Di Cola, A., Frigerio, L., Lord, J. M., Roberts, L. M., and Ceriotti, A. (2005) *Plant Physiol.* **137**, 287–296
- Wiertz, E. J., Jones, T. R., Sun, L., Bogyo, M., Geuze, H. J., and Ploegh, H. L. (1996) *Cell* **84**, 769–779
- Patel, S., and Latterich, M. (1998) *Trends Cell Biol.* **8**, 65–71
- Fiebigler, E., Hirsch, C., Vyas, J. M., Gordon, E., Ploegh, H. L., and Tortorella, D. (2004) *Mol. Biol. Cell* **15**, 1635–1646
- Mueller, B., Klemm, E. J., Spooner, E., Claessen, J. H., and Ploegh, H. L. (2008) *Proc. Natl. Acad. Sci. U.S.A.* **105**, 12325–12330
- Mueller, B., Lilley, B. N., and Ploegh, H. L. (2006) *J. Cell Biol.* **175**, 261–270
- Lilley, B. N., and Ploegh, H. L. (2004) *Nature* **429**, 834–840
- Sun, F., Zhang, R., Gong, X., Geng, X., Drain, P. F., and Frizzell, R. A. (2006) *J. Biol. Chem.* **281**, 36856–36863
- Ye, Y., Shibata, Y., Yun, C., Ron, D., and Rapoport, T. A. (2004) *Nature* **429**, 841–847
- Qu, D., Teckman, J. H., Omura, S., and Perlmutter, D. H. (1996) *J. Biol. Chem.* **271**, 22791–22795
- Teckman, J. H., Qu, D., and Perlmutter, D. H. (1996) *Hepatology* **24**, 1504–1516
- Bernardi, K. M., Forster, M. L., Lencer, W. I., and Tsai, B. (2008) *Mol. Biol. Cell* **19**, 877–884
- London, E., and Luongo, C. L. (1989) *Biochem. Biophys. Res. Commun.* **160**, 333–339
- Deeks, E. D., Cook, J. P., Day, P. J., Smith, D. C., Roberts, L. M., and Lord, J. M. (2002) *Biochemistry* **41**, 3405–3413
- Mayerhofer, P. U., Cook, J. P., Wahlman, J., Pinheiro, T. T., Moore, K. A., Lord, J. M., Johnson, A. E., and Roberts, L. M. (2009) *J. Biol. Chem.* **284**, 10232–10242
- Ploegh, H. L. (2007) *Nature* **448**, 435–438